

CERN-EP-2017-109
2017/10/12

CMS-SUS-16-051

Search for top squark pair production in pp collisions at $\sqrt{s} = 13$ TeV using single lepton events

The CMS Collaboration*

Abstract

A search for top squark pair production in pp collisions at $\sqrt{s} = 13$ TeV is performed using events with a single isolated electron or muon, jets, and a large transverse momentum imbalance. The results are based on data collected in 2016 with the CMS detector at the LHC, corresponding to an integrated luminosity of 35.9 fb^{-1} . No significant excess of events is observed above the expectation from standard model processes. Exclusion limits are set in the context of supersymmetric models of pair production of top squarks that decay either to a top quark and a neutralino or to a bottom quark and a chargino. Depending on the details of the model, we exclude top squarks with masses as high as 1120 GeV. Detailed information is also provided to facilitate theoretical interpretations in other scenarios of physics beyond the standard model.

Published in the Journal of High Energy Physics as doi:10.1007/JHEP10(2017)019.

arXiv:1706.04402v2 [hep-ex] 10 Oct 2017

1 Introduction

Supersymmetry (SUSY) [1–8] is an extension of the standard model (SM) that postulates the existence of a superpartner for every SM particle with the same gauge quantum numbers but differing by one half-unit of spin. The search for a low mass top squark, the scalar partner of the top quark, is of particular interest following the discovery of a Higgs boson [9–11], as it would substantially contribute to the cancellation of the divergent loop corrections to the Higgs boson mass, providing a possible solution to the hierarchy problem [12–14]. We present results of a search for top squark pair production in the final state with a single lepton ($\ell = e$ or μ) with high transverse momentum (p_T), jets, and significant p_T imbalance. Dedicated top squark searches have been carried out by the ATLAS [15] and CMS [16, 17] collaborations based on 13 TeV proton-proton (pp) collisions at the CERN LHC, with data sets corresponding to integrated luminosities of 3.2 and 2.3 fb^{-1} , respectively. In this paper we report on an extension of the search of Ref. [16] in the single-lepton final state that exploits the data sample collected with the CMS detector [18] in 2016, corresponding to the much larger integrated luminosity of 35.9 fb^{-1} . We find no evidence for an excess of events above the expected background from standard model processes, and interpret the results as limits on simplified models [19–22] of the pair production of top squarks (\tilde{t}) decaying into top quarks and neutralinos ($\tilde{\chi}_1^0$) and/or bottom quarks and charginos ($\tilde{\chi}_1^\pm$), as shown in Fig. 1. We take the $\tilde{\chi}_1^0$ to be the lightest supersymmetric particle (LSP) and to be stable.

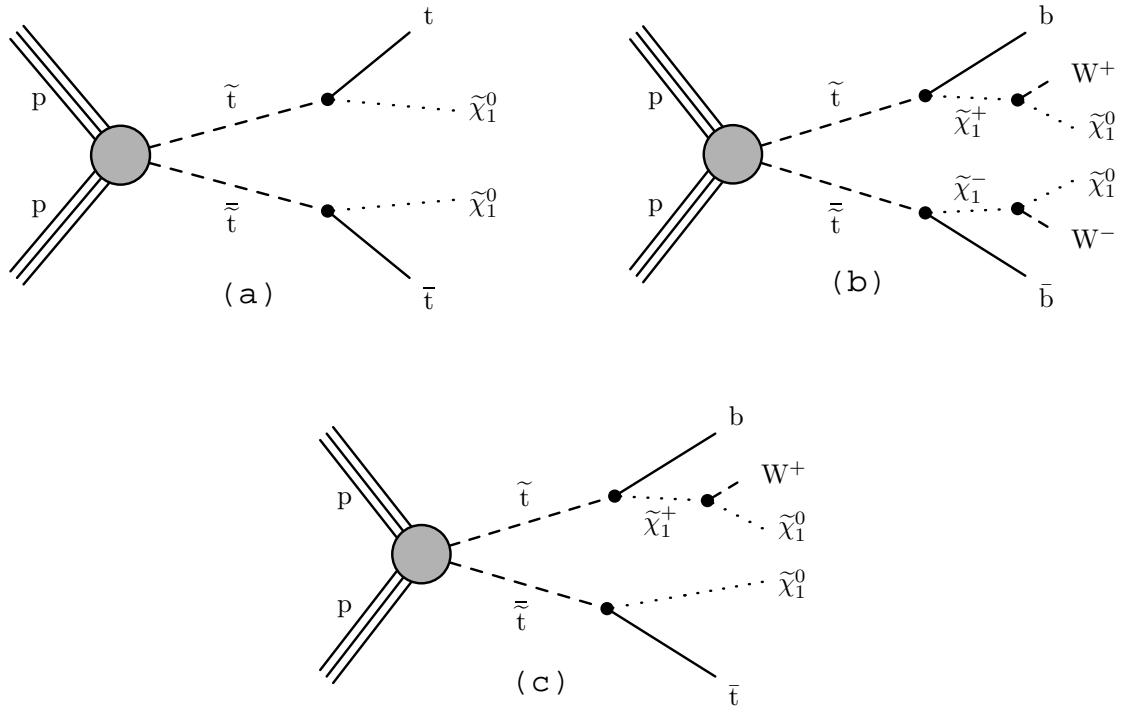


Figure 1: Simplified-models diagrams corresponding to top squark pair production, followed by the specific decay modes targeted in this paper. (a) $pp \rightarrow \tilde{t}\tilde{t}^* \rightarrow t\tilde{\chi}_1^0 \bar{t}\tilde{\chi}_1^0$; (b) $pp \rightarrow \tilde{t}\tilde{t}^* \rightarrow b\tilde{\chi}_1^+ \bar{b}\tilde{\chi}_1^-$; (c) $pp \rightarrow \tilde{t}\tilde{t}^* \rightarrow b\tilde{\chi}_1^+ \bar{t}\tilde{\chi}_1^0$. Charge-conjugate decays are implied.

2 The CMS detector

The central feature of the CMS apparatus is a superconducting solenoid of 6 m internal diameter, providing a magnetic field of 3.8 T. Within the solenoid volume are a silicon pixel and strip tracker, a lead tungstate crystal electromagnetic calorimeter, and a brass and scintillator hadron calorimeter, each composed of a barrel and two endcap sections. Forward calorimeters extend the pseudorapidity (η) coverage provided by the barrel and endcap detectors. Muons are measured in gas-ionization detectors embedded in the steel flux-return yoke outside the solenoid. The first level of the CMS trigger system, composed of custom hardware processors, uses information from the calorimeters and muon detectors to select the most interesting events in a fixed time interval of less than 4 μ s. The high-level trigger processor farm further decreases the event rate from around 100 kHz to less than 1 kHz, before data storage. A more detailed description of the CMS detector, together with a definition of the coordinate system used and the relevant kinematic variables, can be found in Ref. [18].

3 Simulated samples

The Monte Carlo (MC) simulation is used to design the search, to aid in the estimation of SM backgrounds, and to evaluate the sensitivity to top squark pair production.

The MADGRAPH5_aMC@NLO 2.2.2 generator [23] in the leading-order (LO) mode, with MLM matching [24], and with the LO NNPDF3.0 [25] parton distribution functions (PDFs) is used to generate top squark signal events as well as SM $t\bar{t}$, W +jets, Z +jets, and γ +jets. Single top quark events are generated at next-to-leading order (NLO) with POWHEG 2.0 [26–29], while rare SM processes such as $t\bar{t}Z$ and $t\bar{t}W$ are generated at NLO using the MADGRAPH5_aMC@NLO 2.2.2 program, with FxFx matching [30] and the NLO NNPDF3.0 PDFs. Parton showering, hadronization, and the underlying event are modeled by PYTHIA 8.205 [31]. For SM processes, the response of the CMS detector is simulated with the GEANT4 [32] package, while the CMS fast simulation program [33] is used for the signal samples. The most precise cross section calculations are used to normalize the SM simulated samples, corresponding most often to next-to-next-to-leading order (NNLO) accuracy.

To improve on the MADGRAPH5_aMC@NLO modeling of the multiplicity of additional jets from initial state radiation (ISR), simulated $t\bar{t}$ events are reweighted based on the number of ISR jets (N_j^{ISR}) so as to make the jet multiplicity agree with data. The same reweighting procedure is applied to SUSY MC events. The reweighting factors vary between 0.92 and 0.51 for N_j^{ISR} between 1 and 6. We take one half of the deviation from unity as the systematic uncertainty on these reweighting factors to cover possible differences between top quark and top squark pair production.

4 Event reconstruction and preselection

Data events are selected online using triggers that require either a large p_T imbalance or the presence of an isolated electron or muon, see Table 1. The combined trigger efficiency, as measured with a data sample of events with large scalar sum of jet p_T , is $>99\%$ in the signal regions of interest described below.

The offline event reconstruction is based on the particle-flow (PF) algorithm [34], which combines information from the tracker, calorimeter, and muon systems to identify charged and neutral hadrons, photons, electrons, and muons in the event. The preselection based on PF

objects is summarized in Table 1 and is described in more detail below.

The reconstructed vertex with the largest value of summed physics-object p_T^2 is taken to be the primary pp interaction vertex. The physics objects are the objects returned by a jet finding algorithm [35, 36] applied to all charged tracks associated with the vertex, plus the corresponding associated missing transverse momentum.

Selected events are required to have exactly one electron [37] or muon [38] with $p_T > 20$ GeV and $|\eta| < 1.4442$ or $|\eta| < 2.4$, respectively. The lepton needs to be consistent with originating from the primary interaction vertex and isolated from other activity in the event. Typical lepton selection efficiencies are approximately 85% for electrons and 95% for muons within the selection acceptance criteria, with variations at the level of a few percent depending on the p_T and η of the lepton.

Jets are formed by clustering neutral and charged PF objects using the anti- k_T algorithm [35] with a distance parameter of 0.4. The charged PF objects are required to be consistent with originating from the primary vertex. Jet energies are corrected for contributions from multiple interactions in the same or adjacent beam crossings (pileup) [36], and to account for nonuniformity in the detector response [39]. Jets overlapping with the selected lepton within a cone $\Delta R = \sqrt{(\Delta\eta)^2 + (\Delta\phi)^2} = 0.4$ are not considered. We select events with two or more jets with $p_T > 30$ GeV and $|\eta| < 2.4$, at least one of which is required to be consistent with containing the decay of a heavy-flavor hadron. These jets, referred to as b-tagged jets, are identified using two different working points (medium and tight WP) of the CSVv2 tagging algorithm [40, 41]. The jet corrections described above are propagated consistently as a correction to the missing transverse momentum vector (\vec{p}_T^{miss}), defined as the negative vector p_T sum of all PF objects. We denote the magnitude of this vector as E_T^{miss} in the discussion below. Events with possible contributions from beam halo processes or anomalous noise in the calorimeter are rejected using dedicated filters [42].

Background events originating from $t\bar{t}$ decays with only one top quark decaying leptonically ($t\bar{t} \rightarrow 1\ell$), W +jets, and single top quark processes are suppressed by the requirement on the E_T^{miss} and the transverse mass (M_T) of the lepton- \vec{p}_T^{miss} system. For signal, higher values of E_T^{miss} than for background are expected due to the presence of additional unobserved particles, the LSPs. Similarly, the M_T distribution has a jacobian edge around the W boson mass for background events, whereas for signal events no such edge exists due to the presence of the LSPs. We require M_T to be greater than 150 GeV. After these requirements, the largest contribution of SM background events is from processes with two lepton in the final state such as from $t\bar{t}$ ($t\bar{t} \rightarrow 2\ell$) where the second lepton does not pass the selection requirements for the leading lepton. Additional rejection is achieved by vetoing events containing a second lepton or isolated track passing looser identification and isolation requirements than those used for the leading lepton. We also demand that the angle $\min \Delta\phi(J_{1,2}, E_T^{\text{miss}})$ in the azimuthal plane between the \vec{p}_T^{miss} and the direction of the closest of the two leading p_T jets in the event (J_1 and J_2) to be greater than 0.8 radians. This requirement is motivated by the fact that background $t\bar{t} \rightarrow 2\ell$ events tend to have high- p_T top quarks, and thus objects in these events tend to be collinear in the transverse plane, resulting in smaller values of $\min \Delta\phi(J_{1,2}, E_T^{\text{miss}})$ than is typical for signal events.

5 Signal regions

We define two sets of signal regions. The first set (“standard”) is designed to be sensitive to most of the $\Delta m(\tilde{t}, \tilde{\chi}_1^0) \equiv m_{\tilde{t}} - m_{\tilde{\chi}_1^0}$ parameter space, where $m_{\tilde{t}}$ and $m_{\tilde{\chi}_1^0}$ are the masses of the top

Table 1: Summary of the event preselection. The symbol p_T^{lep} denotes the p_T of the lepton, while p_T^{sum} is the scalar p_T sum of PF candidates in a cone around the lepton but excluding the lepton. For veto tracks this variable is calculated using charged PF candidates, while in the case of selected and veto leptons neutral PF candidates are also included. The veto lepton and track definitions are used for event rejection as described in the text. Light-flavor jets are defined as jets originating from u, d, s quarks or gluons.

Trigger	$E_T^{\text{miss}} > 120 \text{ GeV}$ and $H_T^{\text{miss}} = \sum(\vec{p}_T^{\text{jets}}) + \vec{p}_T^{\text{lep}} > 120 \text{ GeV}$ or isolated electron (muon): $p_T^{\text{lep}} > 25(22) \text{ GeV}$, $ \eta < 2.1(2.4)$
Selected lepton	electron (muon): $p_T^{\text{lep}} > 20 \text{ GeV}$, $ \eta < 1.442(2.4)$
Selected lepton isolation	$p_T^{\text{sum}} < 0.1 \times p_T^{\text{lep}}$, $\Delta R = \min[0.2, \max(0.05, 10 \text{ GeV}/p_T^{\text{lep}})]$
Jets and b-tagged jets	$p_T > 30 \text{ GeV}$, $ \eta < 2.4$
b tagging efficiency	medium (tight) WP: 60–70 (35–50)% for jet p_T 30–400 GeV
b tagging mistag rate	medium (tight) WP : $\sim 1\%$ ($\sim 0.2\%$) for light-flavor quarks
Missing transverse momentum	$E_T^{\text{miss}} > 250 \text{ GeV}$ and $\Delta\phi(E_T^{\text{miss}}, J_{1,2}) > 0.8$
Transverse mass	$M_T > 150 \text{ GeV}$
Veto lepton	muon or electron with $p_T^{\text{lep}} > 5 \text{ GeV}$, $ \eta < 2.4$ and $p_T^{\text{sum}} < 0.1 \times p_T^{\text{lep}}$, $\Delta R = \min[0.2, \max(0.05, 10 \text{ GeV}/p_T^{\text{lep}})]$
Veto track	charged PF candidate, $p_T > 10 \text{ GeV}$, $ \eta < 2.4$ and $p_T^{\text{sum}} < \min(0.1 \times p_T^{\text{lep}}, 6 \text{ GeV})$, $\Delta R = 0.3$

squark and the LSP, respectively.

The second set (“compressed”) is designed to enhance sensitivity to the decay mode in Fig. 1(a) when $\Delta m(\tilde{t}, \tilde{\chi}_1^0) \sim m_t$. While the signal regions within each set are mutually exclusive, there is overlap across the signal regions of the two sets.

Both sets have been optimized to have a high signal sensitivity for different decay modes and mass hypotheses using simulation of the SM background processes and the simplified model topologies shown in Fig. 1.

For the first set, signal regions are defined by categorizing events based on the number of jets (N_j), the E_T^{miss} , the invariant mass ($M_{\ell b}$) of the lepton and the closest b-tagged jet in ΔR , and a modified version of the topness variable [43], t_{mod} :

$$t_{\text{mod}} = \ln(\min S), \text{ with } S(\vec{p}_W, p_z, \nu) = \frac{(m_W^2 - (p_\nu + p_\ell)^2)^2}{a_W^4} + \frac{(m_t^2 - (p_b + p_W)^2)^2}{a_t^4} \quad (1)$$

with the constraint $\vec{p}_T^{\text{miss}} = \vec{p}_{T,W} + \vec{p}_{T,\nu}$. The first term corresponds to the leptonically decaying top quark, the second term to the hadronically decaying top quark. The calculation uses resolution parameters $a_W = 5 \text{ GeV}$ and $a_t = 15 \text{ GeV}$. The exact choices of objects used in this variable together with a more detailed motivation can be found in Ref. [16].

In models with \tilde{t} decays containing a $\tilde{\chi}_1^\pm$ that is almost mass degenerate with the $\tilde{\chi}_1^0$, the SM decay products of the $\tilde{\chi}_1^\pm$ are very soft. The final state for these signal can contain a small number of jets, while in signal models without this mass degeneracy at least four jets are expected.

The $M_{\ell b}$ distribution has a sharp endpoint at about $\sqrt{m_t^2 - m_W^2}$ for events containing a leptonically decaying top quark such as $\tilde{t}\bar{t}$ events or signals containing at least one top quark in the decay chain. On the other hand, the $M_{\ell b}$ distribution does not have this endpoint for the subdominant background of W +jets as well as signal models with top squark decays to a b quark and a $\tilde{\chi}_1^\pm$. The t_{mod} variable tests for compatibility with the $\tilde{t}\bar{t} \rightarrow 2\ell$ hypothesis when one of the leptons is not reconstructed. Very high values of t_{mod} imply that an event is not compatible with the $\tilde{t}\bar{t} \rightarrow 2\ell$ hypothesis. Signal models with large $\Delta m(\tilde{t}, \tilde{\chi}_1^0)$ result in such values. On the other hand negative values of t_{mod} are a property of $\tilde{t}\bar{t} \rightarrow 2\ell$. As signal models with a small mass splitting between \tilde{t} and $\tilde{\chi}_1^0$ also have low values in t_{mod} , we keep events with negative t_{mod} , to retain sensitivity for these signal models.

The requirements for the standard signal regions are summarized in Table 2.

Table 2: Definitions for the 27 signal regions of the standard selection. At least one b-tagged jet satisfying the medium WP algorithm is required in all search regions. To suppress the W +jets background in signal regions with $M_{\ell b} > 175 \text{ GeV}$, we instead use the more strict tight WP requirement.

N_j	t_{mod}	$M_{\ell b} [\text{GeV}]$	$E_T^{\text{miss}} [\text{GeV}]$			
2-3	>10	≤ 175	250-350,	350-450,	450-600,	>600
2-3	>10	>175	250-450,	450-600,	>600	
≥4	≤ 0	≤ 175	250-350,	350-450,	450-550,	550-650, >650
≥4	≤ 0	>175	250-350,	350-450,	450-550,	>550
≥4	0-10	≤ 175	250-350,	350-550,	>550	
≥4	0-10	>175	250-450,	>450		
≥4	>10	≤ 175	250-350,	350-450,	450-600,	>600
≥4	>10	>175	250-450,	>450		

The compressed signal regions are designed to select events with a high- p_T jet from ISR, which is needed to provide the necessary boost to the system to obtain large E_T^{miss} and large M_T . Thus, we require at least five jets in the event, with the highest p_T jet failing the medium WP of the b tagging algorithm. Additionally, we reject events if the selected lepton has $p_T > 150$ GeV as we expect the lepton to be soft in the compressed region. We also require the angle between the lepton direction and \vec{p}_T^{miss} in the azimuthal plane to be < 2 . This is because the ISR selection results in boosted top squarks with decay products typically close to each other. Finally, we relax the $\min \Delta\phi(J_{1,2}, E_T^{\text{miss}})$ requirement in the preselection from 0.8 to 0.5 to increase the signal acceptance. The selection requirements for the compressed signal regions are summarized in Table 3.

Table 3: Summary of the compressed selection and the requirements for the four corresponding signal regions. The symbol $\Delta\phi(E_T^{\text{miss}}, \ell)$ denotes the angle between \vec{p}_T^{miss} and the \vec{p}_T^ℓ of the lepton, and J_1 denotes the highest p_T jet.

Selection	$N_j \geq 5$, J_1 not b tagged, $\Delta\phi(E_T^{\text{miss}}, \ell) < 2$, $\min \Delta\phi(J_{1,2}, E_T^{\text{miss}}) > 0.5$, $p_T^\ell < 150$ GeV
Search regions	$E_T^{\text{miss}} = 250\text{-}350, 350\text{-}450, 450\text{-}550, > 550$ GeV

6 Background estimation

Three categories of background from SM processes remain after the selection requirements described in Sections 4 and 5.

- Lost-lepton background: events with two leptonically decaying W bosons in which one of the leptons is not reconstructed or identified. This background arises primarily from $t\bar{t}$ events, with a smaller contribution from single-top quark processes. It is the dominant background in the $M_{\ell b} < 175$ GeV and $N_j \geq 4$ search regions, and is estimated using a dilepton control sample.
- One-lepton background: events with a single leptonically decaying W boson and no additional source of genuine E_T^{miss} . This background is strongly suppressed by the preselection requirements of $E_T^{\text{miss}} > 250$ GeV and $M_T > 150$ GeV.

The suppression is much more effective for events with a W boson originating from the decay of a top quark than for direct W boson production (W+jets), as the mass of the top quark imposes a bound on the mass of the charged lepton-neutrino system. As a result, the tail of the M_T distribution in $t\bar{t} \rightarrow 1\ell$ events is dominated by E_T^{miss} resolution effects, while in W+jets it extends further and is largely driven by the width of the W boson.

The W+jets background estimate is obtained from a control sample of events with no b-tagged jets. The subleading $t\bar{t} \rightarrow 1\ell$ background is modeled from simulation. One-lepton events are the dominant background in the $M_{\ell b} \geq 175$ GeV search regions.

- $Z \rightarrow \nu\bar{\nu}$ background: events with exactly one leptonically decaying W boson and a Z boson that decays to a pair of neutrinos, e.g., $t\bar{t}Z$ or WZ . This background is estimated from simulation, after normalizing the simulated event yield to the observed data counts in a control region obtained by selecting events with three leptons, two of which must be consistent with the Z decay hypothesis.

These three types of backgrounds are discussed below. More details about the validity of the

background estimation methods for the two first categories can be found in Ref. [16].

6.1 Lost-lepton background

The lost-lepton background is estimated from a dilepton control sample obtained with the same selection requirements as the signal sample, except for requiring the presence of a second isolated lepton with $p_T > 10$ GeV. For each signal region, a corresponding control region is constructed, with an exception as noted below. In defining the control regions, the \vec{p}_T of the second lepton is added to the \vec{p}_T^{miss} and all relevant event quantities are recalculated. The estimated background in each search region is then obtained from the yield of data events in the control region and a transfer factor defined as the ratio of the expected SM event yields in the signal and control regions, as determined from simulation. Corrections obtained from studies of $Z/\gamma^* \rightarrow \ell\ell$ events are applied to account for small differences in lepton reconstruction and selection efficiencies between data and simulation.

Due to a lack of statistics, the two or three highest E_T^{miss} bins of Table 2 are combined resulting in the list of control regions listed in Table 4, and the simulation, after the correction described below, is used to determine the expected distribution of SM events as a function of E_T^{miss} . The correction is based on a study of the E_T^{miss} distribution in a top quark enriched control region of $e\mu$ events with at least one b-tagged jet, as shown in Fig. 2. The ratio of data to simulation yields as a function of E_T^{miss} in the $e\mu$ sample is taken as a bin-by-bin correction for the expected E_T^{miss} distribution in the simulation of $t\bar{t}$ and tW events with a lost lepton. The uncertainty in each bin is taken to be one half the deviation from unity.

Table 4: Dilepton control regions utilizing combined bins in E_T^{miss} .

N_j	t_{mod}	$M_{\ell b}$ [GeV]	E_T^{miss} [GeV]
2–3	>10	>175	250-450, 450-600, >600
≥ 4	0–10	≤ 175	350-550, >550
≥ 4	0–10	>175	250-450, >450
≥ 4	>10	>175	250-450, >450

The dominant uncertainties on the transfer factors arise from the statistical uncertainties in the simulated samples and the uncertainties in the lepton efficiency. These range from 5–100% and 5–15%, respectively. The uncertainties on the lepton efficiency are derived from studies of samples of leptonically-decaying Z bosons. For the regions of Table 4, there are also uncertainties associated with the E_T^{miss} distribution. These are also dominated by the statistical precision of the simulated samples, and range between 10 and 100%. Uncertainties due to the jet energy scale and the b tagging efficiency are evaluated by varying the correction factors for simulation by their uncertainties, and the uncertainties due to the choices of renormalization and factorization scale used in the generation of SM samples are assessed by varying the scales by a factor of 2. All these uncertainties are found to be small. The resulting systematic uncertainties on the transfer factors are 10–100%, depending on the region. These are generally smaller than the statistical uncertainties from the data yield in the corresponding control regions that are used, in conjunction with the transfer factors, to predict the SM background in the signal regions.

6.2 One-lepton background

As discussed previously, the one-lepton background receives contributions from processes where the leptonically decaying W boson is produced directly or from the decay of a top quark. The background from direct W boson production is estimated in each search region using a control region obtained with the same selection as the signal region except that the b

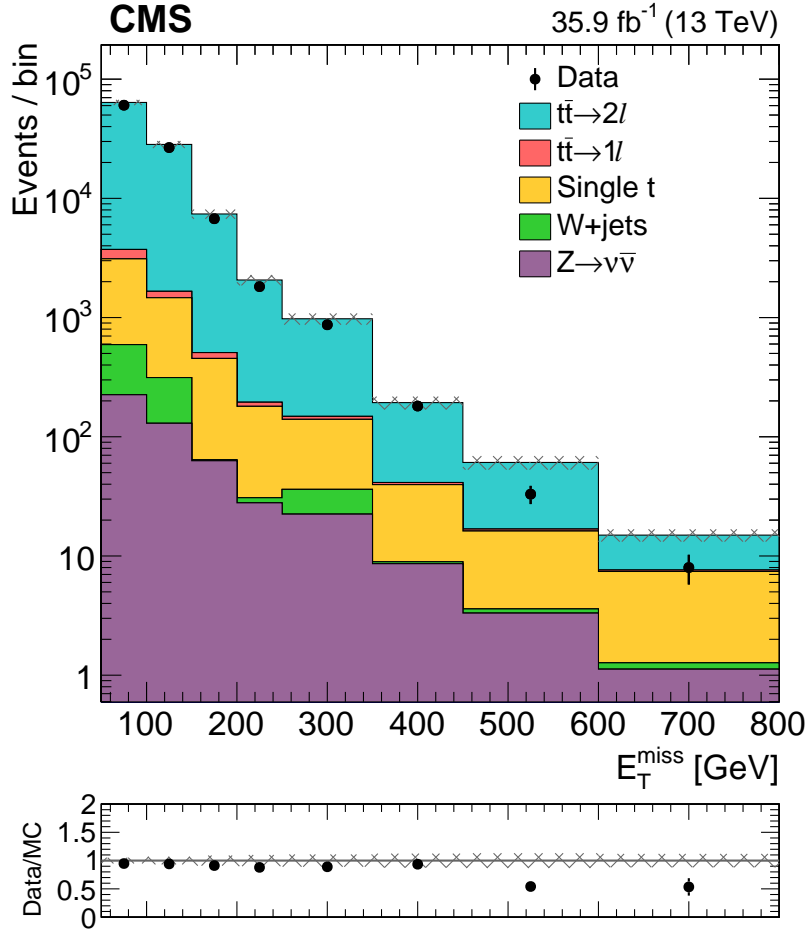


Figure 2: Distributions in E_T^{miss} for a top quark enriched control region of $e\mu$ events with at least one b-tagged jet. The ratio of data to simulation as a function of E_T^{miss} is also shown. It is taken as a correction of the E_T^{miss} distribution in simulation of $t\bar{t}$ and tW events with a lost lepton.

tagging requirement is inverted to enrich the sample in W+jets events. The estimate in each search region is then obtained using a transfer factor determined from simulated samples that accounts for the b quark jet acceptance and tagging efficiency. The estimate is corrected for small differences in the performance of the b tagging algorithm between data and simulation.

In the control sample, the $M_{\ell b}$ variable is constructed using the selected lepton and the jet in the event with the highest value of the b-tag discriminator. The $M_{\ell b}$ distribution is validated in a control sample enriched in the W+jets events, obtained by selecting events with 1 or 2 jets, $60 < M_T < 120 \text{ GeV}$, $E_T^{\text{miss}} > 250 \text{ GeV}$, and either 0 or ≥ 1 jet passing the medium WP of the b tagging algorithm. Figure 3(a) shows the $M_{\ell b}$ distribution in both data and simulation for the control samples with 0 and ≥ 1 b-tagged jets. The bottom panel shows the good agreement between data and simulation in the extrapolation factor from the 0 b-tagged jets sample to the sample with ≥ 1 b-tagged jets.

The largest uncertainty in the transfer factor comes from the limited event counts of the simulated samples, followed by the uncertainty on the heavy-flavor fraction of jets in W+jets events. A comparison of the multiplicity of b-tagged jets between data and simulation is performed in a W+jets enriched region obtained with the same selection as for the $M_{\ell b}$ distribution, as shown

in Fig. 3(b). The difference between data and simulation is covered by a 50% uncertainty on the heavy-flavor component of W +jets events, and is indicated by the shaded band in the figure. Variations of the jet energy scale and b tagging efficiency within their measured uncertainties each result in a 10% uncertainty in the background estimate. The total uncertainty in the estimate of the W +jets background varies from 20 to 80%, depending on signal region.

Simulation studies indicate that in all signal regions the contribution from $t\bar{t} \rightarrow 1\ell$ events is expected to be smaller than 10% of the total background. This estimate is sensitive to the correct modeling of the E_T^{miss} resolution, since this affects the M_T tail. The modeling of the E_T^{miss} resolution is studied using data and simulated samples of γ +jets events. The photon p_T spectrum is reweighted to match that of the neutrino in simulated $t\bar{t} \rightarrow 1\ell$ events after first re-weighting the photon p_T spectrum in simulation to match that observed in data. We then add the photon \vec{p}_T to the E_T^{miss} , and compare the resulting spectra. Differences of up to 40% in the E_T^{miss} shape between data and simulated events are observed, as shown in Fig. 3(c) for a selection with at least 2 jets. Corrections for these differences are applied to the $t\bar{t} \rightarrow 1\ell$ simulation and a resulting 100% uncertainty is assigned to the estimate of this background.

6.3 Background from events containing $Z \rightarrow \nu\bar{\nu}$ decays

The third and last category of background arises from $t\bar{t}Z$, WZ , and other rare multiboson processes, all with a leptonically decaying W boson and one or more Z bosons decaying to neutrinos. Within this category, the contribution from WZ events is dominant in the low- N_j bins, whereas in events with higher N_j , 60–80% of this background is due to $t\bar{t}Z$ processes.

The background from these processes is estimated from simulation with normalization obtained from a data control sample containing three leptons. For this sample, two leptons must form an opposite charge, same flavor pair having an invariant mass between 76 and 106 GeV. The normalization of the WZ and $t\bar{t}Z$ processes is determined by performing a template fit to the distribution of the number of b -tagged jets in this sample. The result of this fit yield scale factors of 1.21 ± 0.11 and 1.14 ± 0.30 to be applied to the simulated samples of WZ and $t\bar{t}Z$ events, respectively.

We also assess all relevant theoretical and experimental uncertainties that can affect the shapes of the kinematic distributions of our signal region definitions by recomputing acceptances after modifying the various kinematical quantities and reconstruction efficiencies within their respective uncertainties. The experimental uncertainties are obtained by variations of the simulation correction factors within their measured uncertainties. The largest contributions are due to the uncertainties in the jet energy scale and to the choices of the renormalization and factorization scales used in the MC generation of SM samples. The latter is obtained by varying the scales by a factor of 2. Other uncertainties are due to the lepton and b tagging efficiencies, the modeling of additional jets in the parton shower, pileup, the value of the strong coupling constant α_S , and the PDF sets. The uncertainty on the PDF sets is evaluated by using replicas of the NNPDF3.0 set [25].

The total uncertainty in the $Z \rightarrow \nu\bar{\nu}$ background is 17–78%, depending on the search region.

7 Results and interpretation

The event yields in data in the 31 search regions defined in Tables 2 and 3 are statistically compatible with the estimated backgrounds from SM processes. They are summarized in Table 5 and Fig. 4 and are interpreted in the context of the simplified models of top squark pair production described in Section 1. Further information on the experimental results to facilitate

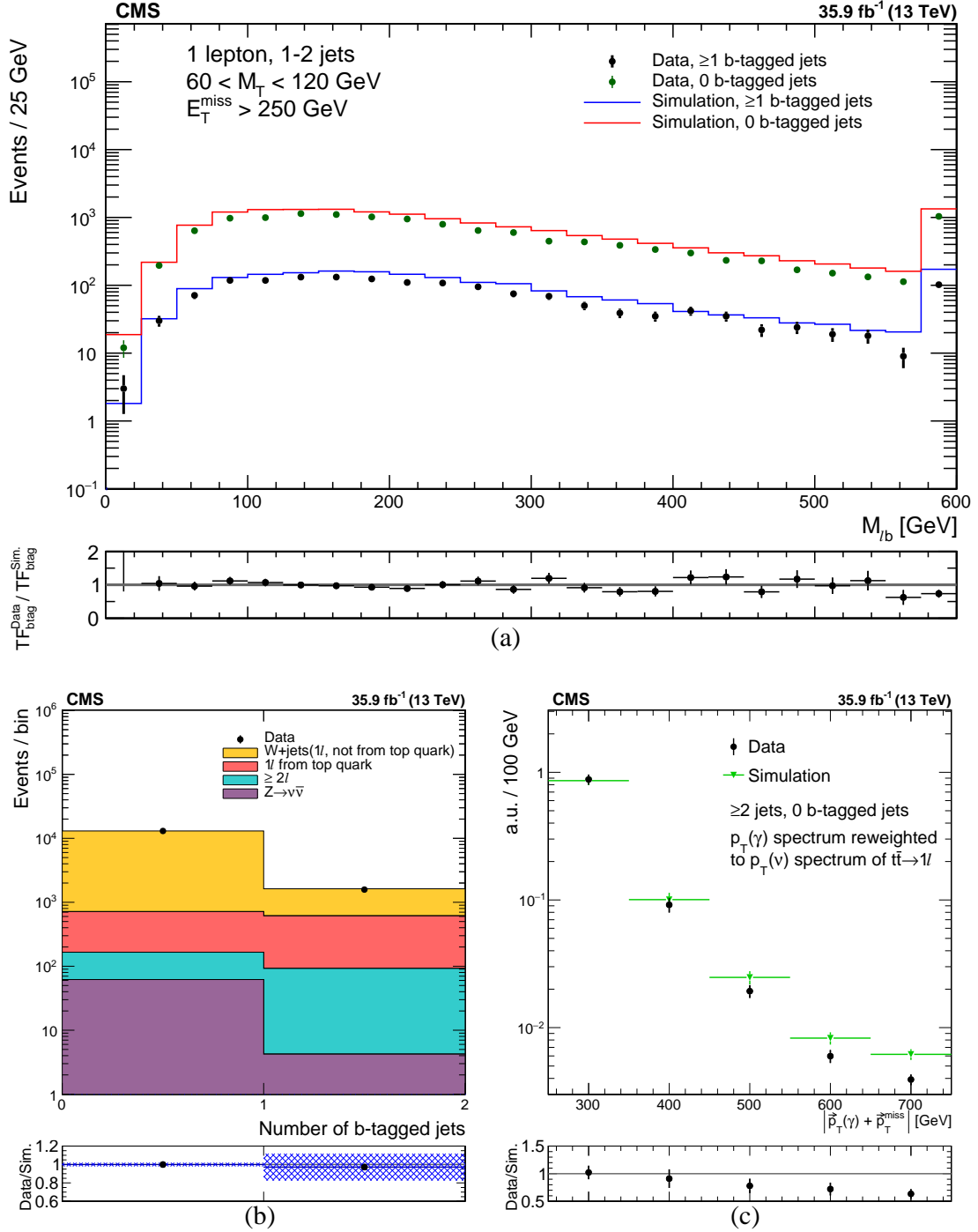


Figure 3: Comparison of the modeling of kinematic distributions in data and simulation relevant for the estimate of the single lepton backgrounds. (a) Distribution in $M_{\ell b}$ in a control sample with 1 or 2 jets, with $60 < M_T < 120$ GeV and $E_T^{\text{miss}} > 250$ GeV. The distribution is shown separately for events with 0 and ≥ 1 jet passing the requirement of the medium b tagging WP. The lower panel shows the ratio of the transfer factors (TF) from the 0 b-tagged jets to the ≥ 1 b-tagged jets samples, in data and simulation. The uncertainty shown is statistical only. (b) Distribution in the number of b-tagged jets in the same control sample. The shaded band shows the uncertainty resulting from a 50% systematic uncertainty in the heavy flavor component of the W +jets sample. (c) Comparison of the E_T^{miss} distribution between data and simulation in the γ +jets control region. The uncertainty shown is statistical only. The ratio between data and simulation shown on the lower panel is used to correct the simulation for its E_T^{miss} resolution.

reinterpretations for beyond the SM models not considered here is given in Appendix A.

Table 5: Result of the background estimates and data yields corresponding to 35.9 fb^{-1} , for the 31 signal regions of Tables 2 and 3.

N_j	t_{mod}	$M_{\ell b}$ [GeV]	$E_{\text{T}}^{\text{miss}}$ [GeV]	Lost lepton	1ℓ (top)	1ℓ (not top)	$Z \rightarrow \nu\bar{\nu}$	Total background	Data
≤ 3	>10	≤ 175	250–350	53.9 ± 6.2	< 0.1	7.2 ± 2.5	4.7 ± 1.2	65.8 ± 6.8	72
≤ 3	>10	≤ 175	350–450	14.2 ± 2.4	0.2 ± 0.2	4.1 ± 1.4	2.1 ± 0.8	20.5 ± 2.9	24
≤ 3	>10	≤ 175	450–600	2.9 ± 0.9	0.1 ± 0.1	1.7 ± 0.7	1.6 ± 0.5	6.4 ± 1.3	6
≤ 3	>10	≤ 175	>600	0.6 ± 0.5	0.3 ± 0.3	0.8 ± 0.3	0.7 ± 0.4	2.4 ± 0.8	2
≤ 3	>10	>175	250–450	1.7 ± 0.8	< 0.1	5.6 ± 2.2	1.5 ± 0.5	8.9 ± 2.4	6
≤ 3	>10	>175	450–600	0.02 ± 0.01	< 0.1	1.6 ± 0.6	0.4 ± 0.3	1.9 ± 0.7	3
≤ 3	>10	>175	>600	0.01 ± 0.01	< 0.1	0.9 ± 0.4	0.1 ± 0.3	1.0 ± 0.5	2
≥ 4	≤ 0	≤ 175	250–350	346 ± 30	13.2 ± 13.2	9.7 ± 8.6	14.4 ± 3.9	383 ± 34	343
≥ 4	≤ 0	≤ 175	350–450	66.3 ± 7.9	2.3 ± 2.3	2.5 ± 1.7	4.4 ± 1.2	75.5 ± 8.5	68
≥ 4	≤ 0	≤ 175	450–550	12.1 ± 2.8	0.6 ± 0.6	0.5 ± 0.5	1.8 ± 0.5	15.0 ± 2.9	13
≥ 4	≤ 0	≤ 175	550–650	3.4 ± 1.5	0.1 ± 0.1	0.3 ± 0.2	0.4 ± 0.1	4.1 ± 1.5	6
≥ 4	≤ 0	≤ 175	>650	5.9 ± 2.8	< 0.1	0.4 ± 0.4	0.2 ± 0.1	6.6 ± 2.9	2
≥ 4	≤ 0	>175	250–350	26.0 ± 4.3	3.1 ± 3.1	7.5 ± 3.0	3.0 ± 0.9	39.7 ± 6.2	38
≥ 4	≤ 0	>175	350–450	10.4 ± 2.6	0.6 ± 0.6	1.6 ± 0.7	1.2 ± 0.4	13.7 ± 2.8	8
≥ 4	≤ 0	>175	450–550	1.7 ± 0.9	0.4 ± 0.4	0.6 ± 0.3	0.5 ± 0.2	3.1 ± 1.1	2
≥ 4	≤ 0	>175	>550	1.1 ± 0.8	< 0.1	1.0 ± 0.6	0.09 ± 0.03	2.2 ± 1.0	1
≥ 4	0–10	≤ 175	250–350	43.0 ± 5.9	1.7 ± 1.7	5.7 ± 3.0	8.3 ± 2.2	58.7 ± 7.2	65
≥ 4	0–10	≤ 175	350–550	9.1 ± 2.0	0.5 ± 0.5	1.2 ± 0.5	3.9 ± 1.1	14.7 ± 2.4	23
≥ 4	0–10	≤ 175	>550	0.6 ± 0.3	0.3 ± 0.3	0.3 ± 0.2	0.3 ± 0.3	1.5 ± 0.6	1
≥ 4	0–10	>175	250–450	4.4 ± 1.4	0.3 ± 0.3	3.1 ± 1.3	1.1 ± 0.3	8.9 ± 1.9	9
≥ 4	0–10	>175	>450	0.10 ± 0.17	< 0.1	0.2 ± 0.3	0.2 ± 0.1	0.6 ± 0.2	0
≥ 4	>10	≤ 175	250–350	9.5 ± 2.3	0.8 ± 0.8	1.1 ± 0.9	3.0 ± 0.8	14.3 ± 2.7	12
≥ 4	>10	≤ 175	350–450	5.9 ± 1.8	0.7 ± 0.7	0.7 ± 0.5	2.7 ± 0.8	10.0 ± 2.1	9
≥ 4	>10	≤ 175	450–600	3.8 ± 1.3	0.1 ± 0.1	0.4 ± 0.3	2.0 ± 0.5	6.3 ± 1.5	3
≥ 4	>10	≤ 175	>600	0.8 ± 0.6	0.7 ± 0.7	0.3 ± 0.4	0.7 ± 0.3	2.4 ± 1.0	0
≥ 4	>10	>175	250–450	0.5 ± 0.3	< 0.1	1.0 ± 0.6	0.4 ± 0.1	1.9 ± 0.7	0
≥ 4	>10	>175	>450	0.2 ± 0.2	0.1 ± 0.1	0.5 ± 0.3	0.5 ± 0.2	1.3 ± 0.4	2
Compressed region			250–350	67.5 ± 8.9	5.3 ± 5.3	5.0 ± 1.8	4.3 ± 1.2	82 ± 11	72
Compressed region			350–450	15.1 ± 3.5	1.0 ± 1.0	0.8 ± 0.3	1.9 ± 0.6	18.9 ± 3.7	30
Compressed region			450–550	2.4 ± 1.3	0.1 ± 0.1	0.4 ± 0.2	0.8 ± 0.3	3.7 ± 1.4	2
Compressed region			>550	3.9 ± 2.0	0.1 ± 0.1	0.2 ± 0.2	0.6 ± 0.2	4.8 ± 2.0	2

For a given model, limits on the production cross-section are derived as a function of the masses of the SUSY particles by combining search regions using a modified frequentist approach, employing the CL_s criterion in an asymptotic formulation [44–47]. These limits are turned into exclusion regions in the $m(\tilde{t}) - m(\tilde{\chi}_1^0)$ plane using the calculation of the cross-section from reference [48] and are shown on Figures 5, 6, and 7. Limits are obtained by combining the 27 regions from the standard selection defined in Table 2, except for the model of Fig. 1(a) in the compressed region $100 \leq \Delta m(\tilde{t}, \tilde{\chi}_1^0) \leq 225 \text{ GeV}$, where we use the four compressed search regions listed in Table 3. This approach improves the expected cross section upper limit in the compressed mass region by $\sim 15\text{--}30\%$. When computing the limits, the expected signal yields are corrected for possible contamination of SUSY events in the data control regions. These corrections are typically around 5–10%.

A summary of the uncertainties in the signal efficiency is shown in Table 6. They are evaluated in the same manner as done in the background estimation methods, described in Section 6. The

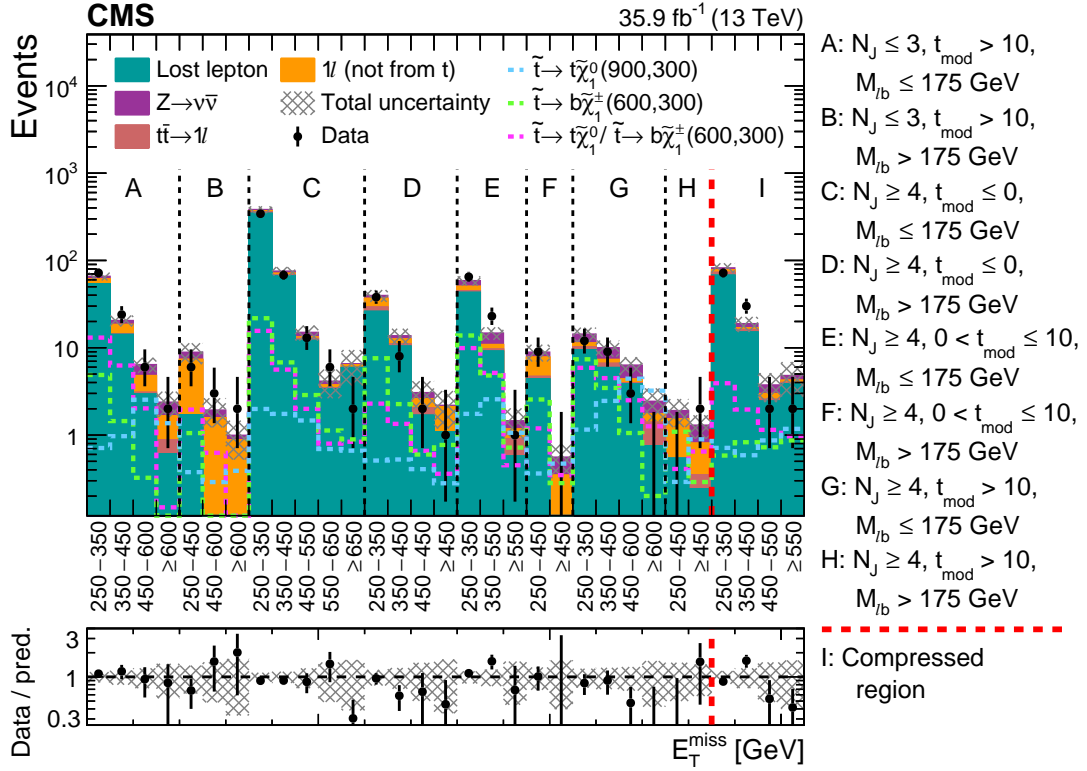


Figure 4: Observed data yields compared with the SM background estimations for the 31 signal regions of Tables 2 and 3. The total uncertainty in the background estimate, determined as the sum in quadrature of statistical and systematic uncertainties, is shown as a shaded band. The expectations for three signal hypotheses are overlaid. The corresponding numbers in parentheses in the legend refer to the masses in GeV of the top squark and the neutralino.

largest uncertainties are due to the limited size of the simulated signal samples, the b tagging efficiency, and the jet energy scale. For model points with a small mass splitting, the ISR uncertainty described in Section 3 is also significant. Since new physics signals are simulated using the CMS fast simulation program, additional uncertainties are assigned to the correction of the lepton and b tagging efficiencies, as well as to cover differences in E_T^{miss} resolution between the fast simulation and the full GEANT4-based model of the CMS detector. The latter uncertainty is small in the bulk of the model space, but may reach up to 25% in scenarios with a compressed mass spectrum. Uncertainties due to the integrated luminosity, ISR modeling, E_T^{miss} resolution, and b tagging and lepton efficiencies are treated as fully correlated across search regions.

Figure 5 shows the 95% confidence level (CL) upper limit on $pp \rightarrow \tilde{t}\tilde{t} \rightarrow \tilde{t}\tilde{\chi}_1^0 \tilde{t}\tilde{\chi}_1^0$, assuming unpolarized top quarks in the decay chain, together with the upper limit at 95% CL on the signal cross section. We exclude top squark masses up to 1120 GeV for a massless LSP and LSP masses up to 515 GeV for a 950 GeV top squark mass. The white band corresponds to the region $|m_{\tilde{t}} - m_t - m_{\tilde{\chi}_1^0}| < 25$ GeV, $m_{\tilde{t}} < 275$ GeV where the selection efficiency of top squark events changes rapidly and becomes very sensitive to details of the model and the simulation. No cross section limit is established in that region.

Figure 6 shows the 95% CL upper limit for $pp \rightarrow \tilde{t}\tilde{t} \rightarrow b\tilde{\chi}_1^\pm \tilde{t}\tilde{\chi}_1^\pm, \tilde{\chi}_1^\pm \rightarrow W\tilde{\chi}_1^0$, together with the upper limit at 95% CL on the excluded signal cross section. The mass of the chargino is chosen to be $(m_{\tilde{t}} + m_{\tilde{\chi}_1^0})/2$. We exclude top squark masses up to 1000 GeV for a massless LSP and LSP masses up to 450 GeV for a 800 GeV top squark mass.

Table 6: Summary of the systematic uncertainties in the signal efficiency.

Source	Typical range of values [%]
Simulation statistical uncertainty	5–25
Renormalization and factorization scales	2–4
Integrated luminosity	2.5
Trigger	2–4
b tagging scale factors	1–7
Jet energy scale	1–20
Lepton identification and veto efficiency	1–4
ISR modeling	2–15
E_T^{miss} modeling	1–10
Total uncertainty	7–38

Figure 7 shows the 95% CL upper limit for $pp \rightarrow \tilde{t}\tilde{t} \rightarrow tb\tilde{\chi}_1^\pm\tilde{\chi}_1^0, \tilde{\chi}_1^\pm \rightarrow W^*\tilde{\chi}_1^0$, together with the upper limit at 95% CL on the excluded signal cross section. The mass splitting of the chargino and neutralino is fixed to 5 GeV. We exclude top squark masses up to 980 GeV for a massless LSP and LSP masses up to 400 GeV for a 825 GeV top squark mass.

8 Summary

We have reported on a search for top squark pair production in pp collisions at $\sqrt{s} = 13$ TeV in events with a single isolated electron or muon, jets, and large missing transverse momentum using data collected with the CMS detector during the 2016 run of the LHC, corresponding to an integrated luminosity of 35.9 fb^{-1} . The event data yields are consistent with the expectations from SM processes. The results are interpreted as exclusion limits in the context of supersymmetric models with pair production of top squarks that decay either to a top quark and a neutralino or to a bottom quark and a chargino. Assuming both top squarks decay to a top quark and a neutralino, we exclude at 95% CL top squark masses up to 1120 GeV for a massless neutralino and neutralino masses up to 515 GeV for a 950 GeV top squark mass. For a scenario where both top squarks decay to a bottom quark and a chargino, with the chargino mass the average of the masses of the neutralino and top squark, we exclude at the 95% CL top squark masses up to 1000 GeV for a massless neutralino and neutralino masses up to 450 GeV for a 800 GeV top squark mass. For the mixed decay scenario, with the mass splitting between the chargino and neutralino fixed to be 5 GeV, we exclude at the 95% CL top squark masses up to 980 GeV for a massless neutralino and neutralino masses up to 400 GeV for a 825 GeV top squark mass.

Acknowledgments

We congratulate our colleagues in the CERN accelerator departments for the excellent performance of the LHC and thank the technical and administrative staffs at CERN and at other CMS institutes for their contributions to the success of the CMS effort. In addition, we gratefully acknowledge the computing centres and personnel of the Worldwide LHC Computing Grid for delivering so effectively the computing infrastructure essential to our analyses. Finally, we acknowledge the enduring support for the construction and operation of the LHC and the CMS detector provided by the following funding agencies: BMFWF and FWF (Austria); FNRS and FWO (Belgium); CNPq, CAPES, FAPERJ, and FAPESP (Brazil); MES (Bulgaria); CERN; CAS, MoST, and NSFC (China); COLCIENCIAS (Colombia); MSES and CSF (Croatia);

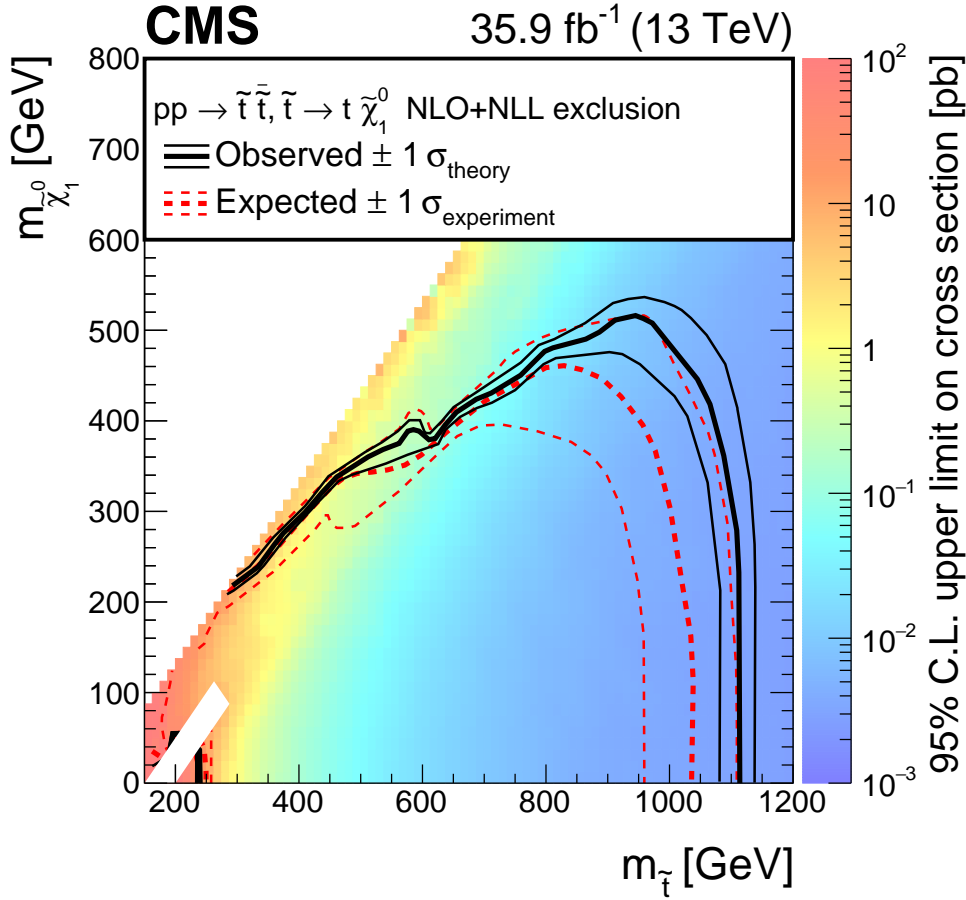


Figure 5: The exclusion limits at 95% CL for direct top squark pair production with decay $\tilde{t}\tilde{t} \rightarrow t\tilde{\chi}_1^0\bar{t}\tilde{\chi}_1^0$. The interpretation is done in the two-dimensional space of $m_{\tilde{t}}$ vs. $m_{\tilde{\chi}_1^0}$. The color indicates the 95% CL upper limit on the cross section times branching fraction at each point in the $m_{\tilde{t}}$ vs. $m_{\tilde{\chi}_1^0}$ plane. The area below the thick black curve represents the observed exclusion region at 95% CL assuming 100% branching fraction, while the dashed red lines indicate the expected limits at 95% CL and their $\pm 1\sigma$ experimental standard deviation uncertainties. The thin black lines show the effect of the theoretical uncertainties (σ_{theory}) in the signal cross section. The whited out region is discussed in Section 7.

RPF (Cyprus); SENESCYT (Ecuador); MoER, ERC IUT, and ERDF (Estonia); Academy of Finland, MEC, and HIP (Finland); CEA and CNRS/IN2P3 (France); BMBF, DFG, and HGF (Germany); GSRT (Greece); OTKA and NIH (Hungary); DAE and DST (India); IPM (Iran); SFI (Ireland); INFN (Italy); MSIP and NRF (Republic of Korea); LAS (Lithuania); MOE and UM (Malaysia); BUAP, CINVESTAV, CONACYT, LNS, SEP, and UASLP-FAI (Mexico); MBIE (New Zealand); PAEC (Pakistan); MSHE and NSC (Poland); FCT (Portugal); JINR (Dubna); MON, RosAtom, RAS, RFBR and RAEP (Russia); MESTD (Serbia); SEIDI, CPAN, PCTI and FEDER (Spain); Swiss Funding Agencies (Switzerland); MST (Taipei); ThEPCenter, IPST, STAR, and NSTDA (Thailand); TUBITAK and TAEK (Turkey); NASU and SFFR (Ukraine); STFC (United Kingdom); DOE and NSF (USA).

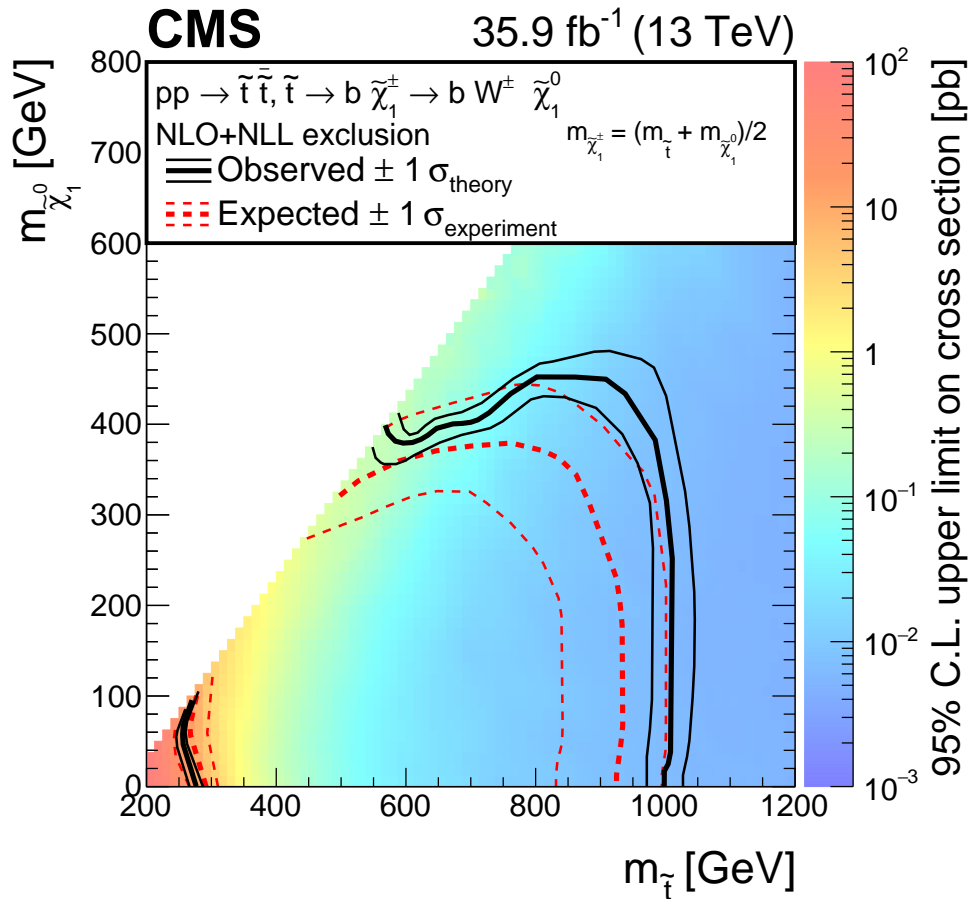


Figure 6: The exclusion limit at 95% CL for direct top squark pair production with decay $\tilde{t}\tilde{t}^* \rightarrow b\tilde{\chi}_1^+\bar{b}\tilde{\chi}_1^-$, $\tilde{\chi}_1^\pm \rightarrow W^\pm\tilde{\chi}_1^0$. The mass of the chargino is chosen to be $(m_{\tilde{t}} + m_{\tilde{\chi}_1^0})/2$. The interpretation is done in the two-dimensional space of $m_{\tilde{t}}$ vs. $m_{\tilde{\chi}_1^0}$. The color indicates the 95% CL upper limit on the cross section times branching fraction at each point in the $m_{\tilde{t}}$ vs. $m_{\tilde{\chi}_1^0}$ plane. The area between the thick black curves represents the observed exclusion region at 95% CL assuming 100% branching fraction, while the dashed red lines indicate the expected limits at 95% CL and their $\pm 1\sigma$ experimental standard deviation uncertainties. The thin black lines show the effect of the theoretical uncertainties (σ_{theory}) in the signal cross section.

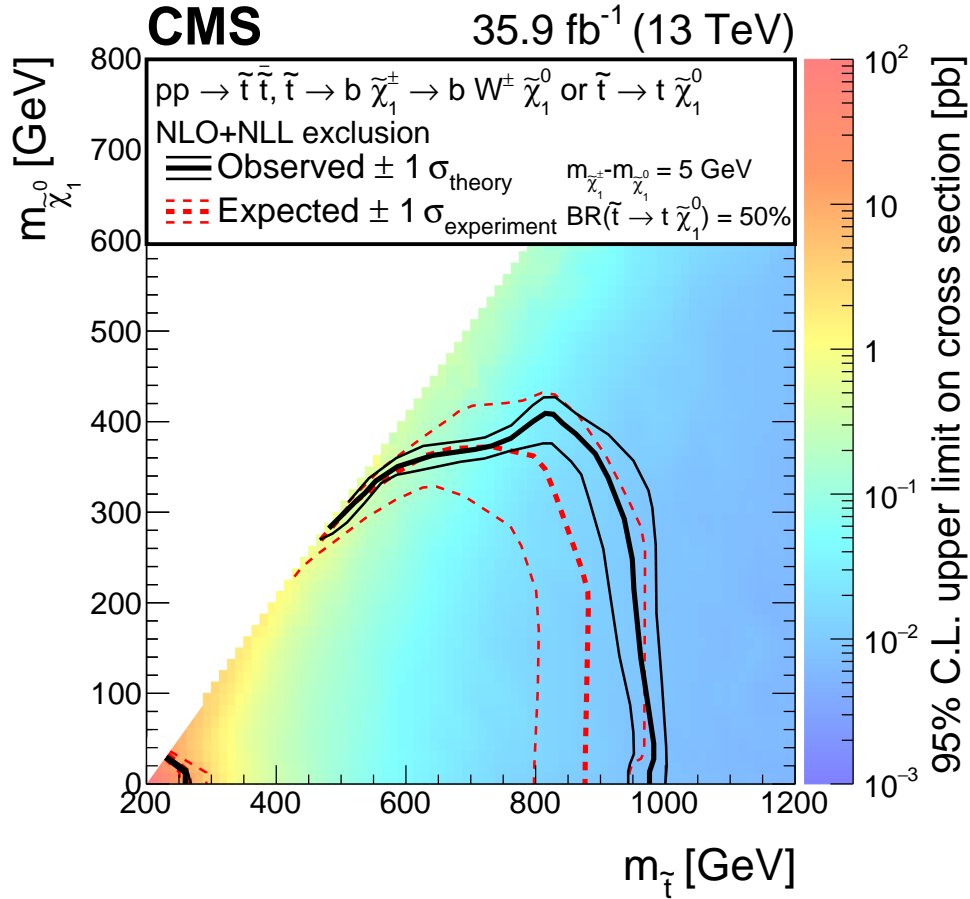


Figure 7: The exclusion limit at 95% CL for direct top squark pair production with decay $\tilde{t} \tilde{t}^* \rightarrow b \tilde{\chi}_1^+ \tilde{\chi}_1^0, \tilde{\chi}_1^\pm \rightarrow W^\pm \tilde{\chi}_1^0$. The mass splitting of the chargino and neutralino is fixed to 5 GeV. The interpretation is done in the two-dimensional space of $m_{\tilde{t}}$ vs. $m_{\tilde{\chi}_1^0}$. The color indicates the 95% CL upper limit on the cross section at each point in the $m_{\tilde{t}}$ vs. $m_{\tilde{\chi}_1^0}$ plane. The area between the thick black curves represents the observed exclusion region at 95% CL, while the dashed red lines indicate the expected limits at 95% CL and their $\pm 1\sigma$ experimental standard deviation uncertainties. The thin black lines show the effect of the theoretical uncertainties (σ_{theory}) in the signal cross section.

References

- [1] P. Ramond, "Dual theory for free fermions", *Phys. Rev. D* **3** (1971) 2415, doi:10.1103/PhysRevD.3.2415.
- [2] Y. A. Golfand and E. P. Likhtman, "Extension of the algebra of Poincaré group generators and violation of P invariance", *JETP Lett.* **13** (1971) 323.
- [3] A. Neveu and J. H. Schwarz, "Factorizable dual model of pions", *Nucl. Phys. B* **31** (1971) 86, doi:10.1016/0550-3213(71)90448-2.
- [4] D. V. Volkov and V. P. Akulov, "Possible universal neutrino interaction", *JETP Lett.* **16** (1972) 438.
- [5] J. Wess and B. Zumino, "A Lagrangian model invariant under supergauge transformations", *Phys. Lett. B* **49** (1974) 52, doi:10.1016/0370-2693(74)90578-4.
- [6] J. Wess and B. Zumino, "Supergauge transformations in four dimensions", *Nucl. Phys. B* **70** (1974) 39, doi:10.1016/0550-3213(74)90355-1.
- [7] P. Fayet, "Supergauge invariant extension of the Higgs mechanism and a model for the electron and its neutrino", *Nucl. Phys. B* **90** (1975) 104, doi:10.1016/0550-3213(75)90636-7.
- [8] H. P. Nilles, "Supersymmetry, supergravity and particle physics", *Phys. Rep.* **110** (1984) 1, doi:10.1016/0370-1573(84)90008-5.
- [9] ATLAS Collaboration, "Observation of a new particle in the search for the Standard Model Higgs boson with the ATLAS detector at the LHC", *Phys. Lett. B* **716** (2012) 1, doi:10.1016/j.physletb.2012.08.020, arXiv:1207.7214.
- [10] CMS Collaboration, "Observation of a new boson at a mass of 125 GeV with the CMS experiment at the LHC", *Phys. Lett. B* **716** (2012) 30, doi:10.1016/j.physletb.2012.08.021, arXiv:1207.7235.
- [11] CMS Collaboration, "Combined results of searches for the standard model Higgs boson in pp collisions at $\sqrt{s} = 7$ TeV", *Phys. Lett. B* **710** (2012) 26, doi:10.1016/j.physletb.2012.02.064, arXiv:1202.1488.
- [12] M. Papucci, J. T. Ruderman, and A. Weiler, "Natural SUSY endures", *JHEP* **09** (2012) 035, doi:10.1007/JHEP09(2012)035, arXiv:1110.6926.
- [13] R. Barbieri and D. Pappadopulo, "S-particles at their naturalness limits", *JHEP* **10** (2009) 061, doi:10.1088/1126-6708/2009/10/061, arXiv:0906.4546.
- [14] S. Dimopoulos and G. F. Giudice, "Naturalness constraints in supersymmetric theories with nonuniversal soft terms", *Phys. Lett. B* **357** (1995) 573, doi:10.1016/0370-2693(95)00961-J, arXiv:hep-ph/9507282.
- [15] ATLAS Collaboration, "Search for top squarks in final states with one isolated lepton, jets, and missing transverse momentum in $\sqrt{s} = 13$ TeV pp collisions with the ATLAS detector", *Phys. Rev. D* **94** (2016) 052009, doi:10.1103/PhysRevD.94.052009, arXiv:1606.03903.

- [16] CMS Collaboration, “Searches for pair production of third-generation squarks in $\sqrt{s} = 13$ TeV pp collisions”, *Eur. Phys. J. C* **77** (2017) 327, doi:10.1140/epjc/s10052-017-4853-2, arXiv:1612.03877.
- [17] CMS Collaboration, “Search for supersymmetry in the all-hadronic final state using top quark tagging in pp collisions at $\sqrt{s} = 13$ TeV”, *Phys. Rev. D* **96** (2017) 012004, doi:10.1103/PhysRevD.96.012004, arXiv:1701.01954.
- [18] CMS Collaboration, “The CMS experiment at the CERN LHC”, *JINST* **3** (2008) S08004, doi:10.1088/1748-0221/3/08/S08004.
- [19] N. Arkani-Hamed et al., “MARMOSET: the path from LHC data to the new standard model via on-shell effective theories”, (2007). arXiv:hep-ph/0703088.
- [20] J. Alwall, P. Schuster, and N. Toro, “Simplified models for a first characterization of new physics at the LHC”, *Phys. Rev. D* **79** (2009) 075020, doi:10.1103/PhysRevD.79.075020, arXiv:0810.3921.
- [21] J. Alwall, M.-P. Le, M. Lisanti, and J. G. Wacker, “Model-independent jets plus missing energy searches”, *Phys. Rev. D* **79** (2009) 015005, doi:10.1103/PhysRevD.79.015005, arXiv:0809.3264.
- [22] LHC New Physics Working Group Collaboration, “Simplified models for LHC new physics searches”, *J. Phys. G* **39** (2012) 105005, doi:10.1088/0954-3899/39/10/105005, arXiv:1105.2838.
- [23] J. Alwall et al., “The automated computation of tree-level and next-to-leading order differential cross sections, and their matching to parton shower simulations”, *JHEP* **07** (2014) 079, doi:10.1007/JHEP07(2014)079, arXiv:1405.0301.
- [24] J. Alwall et al., “Comparative study of various algorithms for the merging of parton showers and matrix elements in hadronic collisions”, *Eur. Phys. J. C* **53** (2008) 473, doi:10.1140/epjc/s10052-007-0490-5, arXiv:0706.2569.
- [25] NNPDF Collaboration, “Parton distributions for the LHC Run II”, *JHEP* **04** (2015) 040, doi:10.1007/JHEP04(2015)040, arXiv:1410.8849.
- [26] P. Nason, “A new method for combining NLO QCD with shower Monte Carlo algorithms”, *JHEP* **11** (2004) 040, doi:10.1088/1126-6708/2004/11/040, arXiv:hep-ph/0409146.
- [27] S. Frixione, P. Nason, and C. Oleari, “Matching NLO QCD computations with parton shower simulations: the POWHEG method”, *JHEP* **11** (2007) 070, doi:10.1088/1126-6708/2007/11/070, arXiv:0709.2092.
- [28] S. Alioli, P. Nason, C. Oleari, and E. Re, “A general framework for implementing NLO calculations in shower Monte Carlo programs: the POWHEG BOX”, *JHEP* **06** (2010) 043, doi:10.1007/JHEP06(2010)043, arXiv:1002.2581.
- [29] E. Re, “Single-top Wt -channel production matched with parton showers using the POWHEG method”, *Eur. Phys. J. C* **71** (2011) 1547, doi:10.1140/epjc/s10052-011-1547-z, arXiv:1009.2450.
- [30] R. Frederix and S. Frixione, “Merging meets matching in MC@NLO”, *JHEP* **12** (2012) 061, doi:10.1007/JHEP12(2012)061, arXiv:1209.6215.

- [31] T. Sjöstrand et al., “An introduction to PYTHIA 8.2”, *Comput. Phys. Commun.* **191** (2015) 159, doi:10.1016/j.cpc.2015.01.024, arXiv:1410.3012.
- [32] GEANT4 Collaboration, “GEANT4—a simulation toolkit”, *Nucl. Instrum. Meth. A* **506** (2003) 250, doi:10.1016/S0168-9002(03)01368-8.
- [33] S. Abdullin et al., “The fast simulation of the CMS detector at LHC”, *J. Phys. Conf. Ser.* **331** (2011) 032049, doi:10.1088/1742-6596/331/3/032049.
- [34] CMS Collaboration, “Particle-flow reconstruction and global event description with the CMS detector”, (2017). arXiv:1706.04965. Submitted to *JINST*.
- [35] M. Cacciari, G. P. Salam, and G. Soyez, “The anti- k_t jet clustering algorithm”, *JHEP* **04** (2008) 063, doi:10.1088/1126-6708/2008/04/063, arXiv:0802.1189.
- [36] M. Cacciari, G. P. Salam, and G. Soyez, “FastJet user manual”, *Eur. Phys. J. C* **72** (2012) 1896, doi:10.1140/epjc/s10052-012-1896-2, arXiv:1111.6097.
- [37] CMS Collaboration, “Performance of electron reconstruction and selection with the cms detector in proton-proton collisions at $\sqrt{s} = 8$ tev”, *JINST* **10** (2015) P06005, doi:10.1088/1748-0221/10/06/P06005, arXiv:1502.02701.
- [38] CMS Collaboration, “Performance of CMS muon reconstruction in pp collision events at $\sqrt{s} = 7$ TeV”, *JINST* **7** (2012) P10002, doi:10.1088/1748-0221/7/10/P10002, arXiv:1206.4071.
- [39] CMS Collaboration, “Jet energy scale and resolution in the CMS experiment in pp collisions at 8 TeV”, *JINST* **12** (2017) P02014, doi:10.1088/1748-0221/12/02/P02014, arXiv:1607.03663.
- [40] CMS Collaboration, “Identification of b-quark jets with the CMS experiment”, *JINST* **8** (2013) P04013, doi:10.1088/1748-0221/8/04/P04013, arXiv:1211.4462.
- [41] CMS Collaboration, “Identification of b quark jets at the CMS experiment in the LHC run 2”, CMS Physics Analysis Summary CMS-PAS-BTV-15-001, 2016.
- [42] CMS Collaboration, “Missing transverse energy performance of the CMS detector”, *JINST* **6** (2011) P09001, doi:10.1088/1748-0221/6/09/P09001, arXiv:1106.5048.
- [43] M. L. Graesser and J. Shelton, “Hunting mixed top squark decays”, *Phys. Rev. Lett.* **111** (2013) 121802, doi:10.1103/PhysRevLett.111.121802, arXiv:1212.4495.
- [44] T. Junk, “Confidence level computation for combining searches with small statistics”, *Nucl. Instrum. Meth. A* **434** (1999) 435, doi:10.1016/S0168-9002(99)00498-2, arXiv:hep-ex/9902006.
- [45] A. L. Read, “Presentation of search results: the CL_s technique”, *J. Phys. G* **28** (2002) 2693, doi:10.1088/0954-3899/28/10/313.
- [46] G. Cowan, K. Cranmer, E. Gross, and O. Vitells, “Asymptotic formulae for likelihood-based tests of new physics”, *Eur. Phys. J. C* **71** (2011) 1554, doi:10.1140/epjc/s10052-011-1554-0, arXiv:1007.1727. [Erratum: doi:10.1140/epjc/s10052-013-2501-z].

-
- [47] ATLAS and CMS Collaborations, LHC Higgs Combination Group, “Procedure for the LHC Higgs boson search combination in Summer 2011”, Technical Report ATL-PHYS-PUB 2011-11, CMS NOTE 2011/005, 2011.
- [48] C. Borschensky et al., “Squark and gluino production cross sections in pp collisions at $\sqrt{s} = 13, 14, 33$ and 100 TeV”, *Eur. Phys. J. C* **74** (2014) 3174, doi:10.1140/epjc/s10052-014-3174-y, arXiv:1407.5066.
- [49] CMS Collaboration, “Simplified likelihood for the re-interpretation of public CMS results”, Technical Report CERN-CMS-NOTE-2017-001, CERN, Geneva, 2017.

A Additional information

The yields and background predictions of this search can be used to confront scenarios for physics beyond the standard model (BSM) not considered in this paper. To facilitate such reinterpretations, in Table 7 we provide results for a small number of inclusive aggregated signal regions. The background expectation, the event count, and the expected BSM yield in any one of these regions can be used to constrain BSM hypotheses in a simple way. In addition, we provide the correlation matrix for the background predictions in the full set of search regions (Figs. 8 and 9). This information can be used to exploit the full power of the analysis by constructing a simplified likelihood for a BSM model as described in Ref. [49].

Table 7: Background predictions and yields in data corresponding to 35.9 fb^{-1} for aggregate signal regions.

N_j	t_{mod}	$M_{\ell b}$ [GeV]	E_T^{miss} [GeV]	Lost lepton	1ℓ (top)	1ℓ (not top)	$Z \rightarrow \nu\bar{\nu}$	Total background	Data
≤ 3	> 10		> 600	0.6 ± 0.5	0.3 ± 0.3	1.7 ± 0.5	0.8 ± 0.5	3.4 ± 0.9	4
≥ 4	≤ 0	≤ 175	> 550	9.3 ± 3.2	0.1 ± 0.1	0.7 ± 0.4	0.6 ± 0.1	10.7 ± 3.2	8
≥ 4	> 10	≤ 175	> 450	4.6 ± 1.4	0.8 ± 0.7	0.8 ± 0.5	2.7 ± 0.6	8.8 ± 1.8	3
≥ 4	≤ 0	> 175	> 450	2.8 ± 1.2	0.4 ± 0.4	1.6 ± 0.7	0.5 ± 0.3	5.3 ± 1.5	3
≥ 4	> 0	> 175	> 450	0.3 ± 0.2	0.1 ± 0.1	0.7 ± 0.3	0.7 ± 0.2	1.9 ± 0.5	2
compressed region			> 450	6.3 ± 2.4	0.3 ± 0.2	0.7 ± 0.3	1.3 ± 0.3	8.6 ± 2.5	4

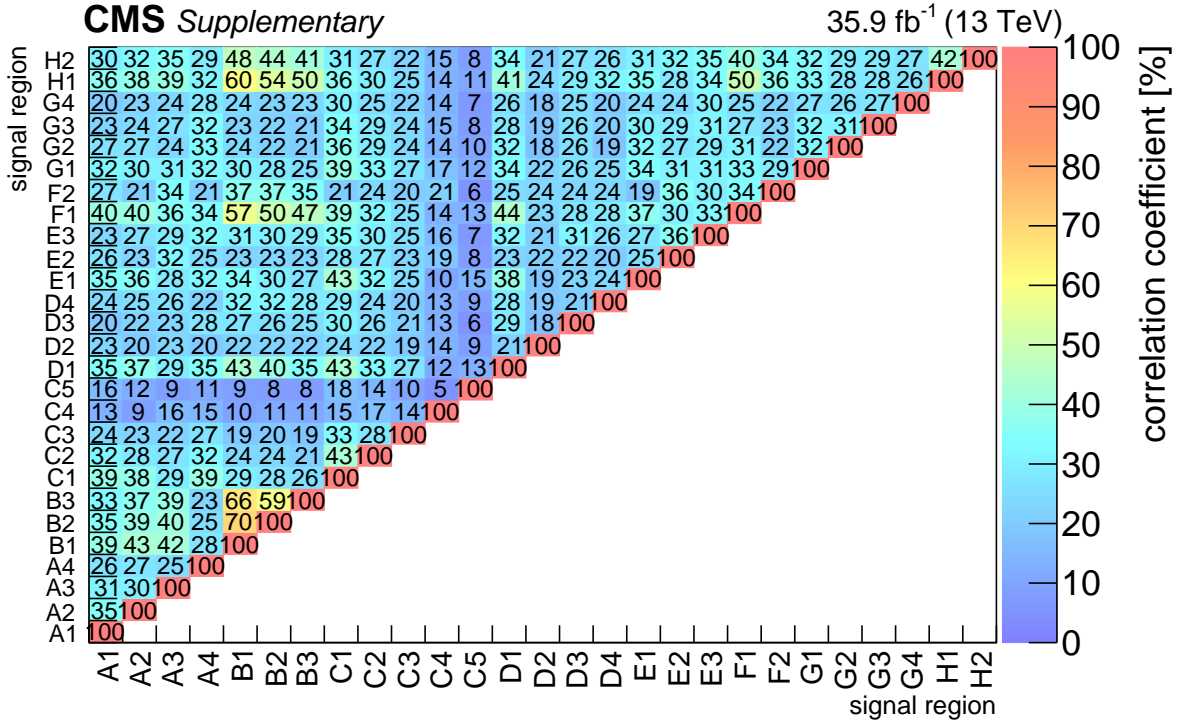


Figure 8: Correlation matrix for the background predictions for the signal regions for the standard selection (in percent). The labelling of the regions follows the convention of Fig. 4.

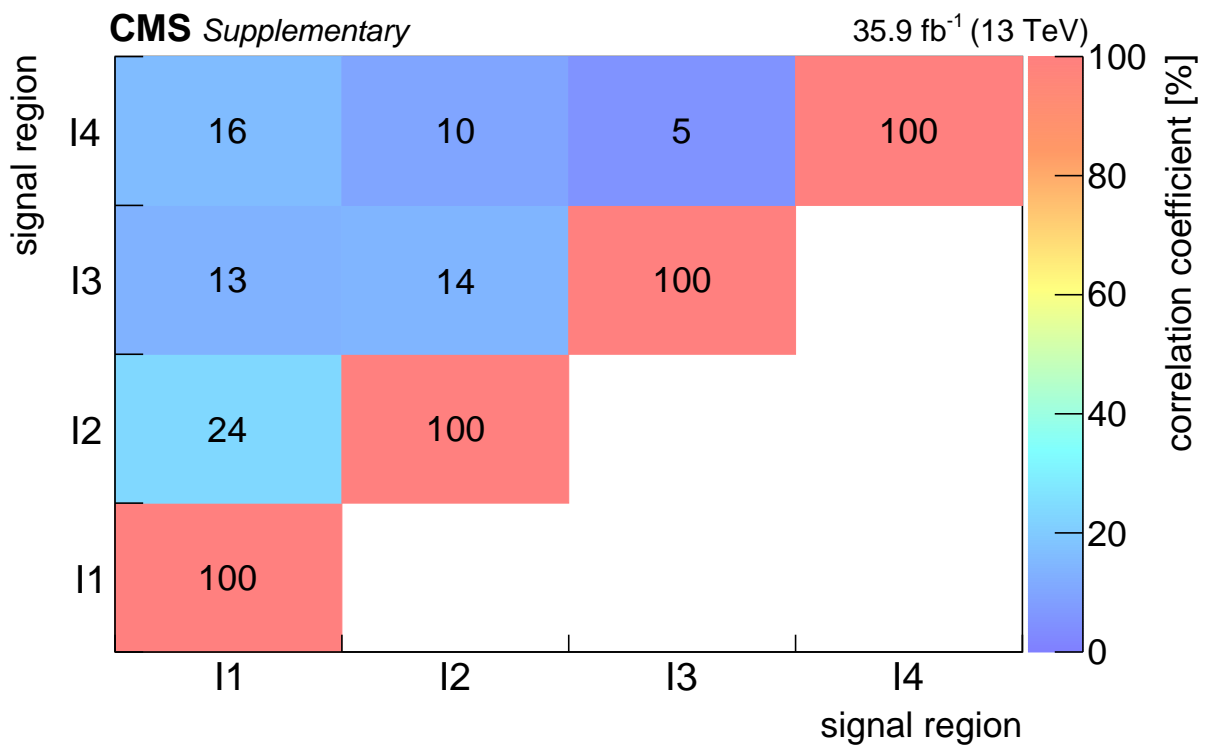


Figure 9: Correlation matrix for the background predictions for the signal regions for the compressed selection (in percent). The labelling of the regions follows the convention of Fig. 4.

B The CMS Collaboration

Yerevan Physics Institute, Yerevan, Armenia

A.M. Sirunyan, A. Tumasyan

Institut für Hochenergiephysik, Wien, Austria

W. Adam, F. Ambrogio, E. Asilar, T. Bergauer, J. Brandstetter, E. Brondolin, M. Dragicevic, J. Erö, M. Flechl, M. Friedl, R. Frühwirth¹, V.M. Ghete, J. Grossmann, J. Hrubec, M. Jeitler¹, A. König, N. Krammer, I. Krätschmer, D. Liko, T. Madlener, I. Mikulec, E. Pree, D. Rabady, N. Rad, H. Rohringer, J. Schieck¹, R. Schöfbeck, M. Spanring, D. Spitzbart, J. Strauss, W. Waltenberger, J. Wittmann, C.-E. Wulz¹, M. Zarucki

Institute for Nuclear Problems, Minsk, Belarus

V. Chekhovsky, V. Mossolov, J. Suarez Gonzalez

Universiteit Antwerpen, Antwerpen, Belgium

E.A. De Wolf, D. Di Croce, X. Janssen, J. Lauwers, H. Van Haevermaet, P. Van Mechelen, N. Van Remortel

Vrije Universiteit Brussel, Brussel, Belgium

S. Abu Zeid, F. Blekman, J. D'Hondt, I. De Bruyn, J. De Clercq, K. Deroover, G. Flouris, D. Lontkovskyi, S. Lowette, S. Moortgat, L. Moreels, A. Olbrechts, Q. Python, K. Skovpen, S. Tavernier, W. Van Doninck, P. Van Mulders, I. Van Parijs

Université Libre de Bruxelles, Bruxelles, Belgium

H. Brun, B. Clerbaux, G. De Lentdecker, H. Delannoy, G. Fasanella, L. Favart, R. Goldouzian, A. Grebenyuk, G. Karapostoli, T. Lenzi, J. Luetic, T. Maerschalk, A. Marinov, A. Randle-conde, T. Seva, C. Vander Velde, P. Vanlaer, D. Vannerom, R. Yonamine, F. Zenoni, F. Zhang²

Ghent University, Ghent, Belgium

A. Cimmino, T. Cornelis, D. Dobur, A. Fagot, M. Gul, I. Khvastunov, D. Poyraz, C. Roskas, S. Salva, M. Tytgat, W. Verbeke, N. Zaganidis

Université Catholique de Louvain, Louvain-la-Neuve, Belgium

H. Bakhshiansohi, O. Bondu, S. Brochet, G. Bruno, A. Caudron, S. De Visscher, C. Delaere, M. Delcourt, B. Francois, A. Giammanco, A. Jafari, M. Komm, G. Krintiras, V. Lemaitre, A. Magitteri, A. Mertens, M. Musich, K. Piotrkowski, L. Quertenmont, M. Vidal Marono, S. Wertz

Université de Mons, Mons, Belgium

N. Bely

Centro Brasileiro de Pesquisas Fisicas, Rio de Janeiro, Brazil

W.L. Aldá Júnior, F.L. Alves, G.A. Alves, L. Brito, M. Correa Martins Junior, C. Hensel, A. Moraes, M.E. Pol, P. Rebello Teles

Universidade do Estado do Rio de Janeiro, Rio de Janeiro, Brazil

E. Belchior Batista Das Chagas, W. Carvalho, J. Chinellato³, A. Custódio, E.M. Da Costa, G.G. Da Silveira⁴, D. De Jesus Damiao, S. Fonseca De Souza, L.M. Huertas Guativa, H. Malbouisson, M. Melo De Almeida, C. Mora Herrera, L. Mundim, H. Nogima, A. Santoro, A. Sznajder, E.J. Tonelli Manganote³, F. Torres Da Silva De Araujo, A. Vilela Pereira

Universidade Estadual Paulista ^a, Universidade Federal do ABC ^b, São Paulo, Brazil

S. Ahuja^a, C.A. Bernardes^a, T.R. Fernandez Perez Tomei^a, E.M. Gregores^b, P.G. Mercadante^b, S.F. Novaes^a, Sandra S. Padula^a, D. Romero Abad^b, J.C. Ruiz Vargas^a

Institute for Nuclear Research and Nuclear Energy of Bulgaria Academy of Sciences

A. Aleksandrov, R. Hadjiiska, P. Iaydjiev, M. Misheva, M. Rodozov, M. Shopova, S. Stoykova, G. Sultanov

University of Sofia, Sofia, Bulgaria

A. Dimitrov, I. Glushkov, L. Litov, B. Pavlov, P. Petkov

Beihang University, Beijing, China

W. Fang⁵, X. Gao⁵

Institute of High Energy Physics, Beijing, China

M. Ahmad, J.G. Bian, G.M. Chen, H.S. Chen, M. Chen, Y. Chen, C.H. Jiang, D. Leggat, H. Liao, Z. Liu, F. Romeo, S.M. Shaheen, A. Spiezia, J. Tao, C. Wang, Z. Wang, E. Yazgan, H. Zhang, J. Zhao

State Key Laboratory of Nuclear Physics and Technology, Peking University, Beijing, China

Y. Ban, G. Chen, Q. Li, S. Liu, Y. Mao, S.J. Qian, D. Wang, Z. Xu

Universidad de Los Andes, Bogota, Colombia

C. Avila, A. Cabrera, L.F. Chaparro Sierra, C. Florez, C.F. González Hernández, J.D. Ruiz Alvarez

University of Split, Faculty of Electrical Engineering, Mechanical Engineering and Naval Architecture, Split, Croatia

B. Courbon, N. Godinovic, D. Lelas, I. Puljak, P.M. Ribeiro Cipriano, T. Sculac

University of Split, Faculty of Science, Split, Croatia

Z. Antunovic, M. Kovac

Institute Rudjer Boskovic, Zagreb, Croatia

V. Brigljevic, D. Ferencek, K. Kadija, B. Mesic, A. Starodumov⁶, T. Susa

University of Cyprus, Nicosia, Cyprus

M.W. Ather, A. Attikis, G. Mavromanolakis, J. Mousa, C. Nicolaou, F. Ptochos, P.A. Razis, H. Rykaczewski

Charles University, Prague, Czech Republic

M. Finger⁷, M. Finger Jr.⁷

Universidad San Francisco de Quito, Quito, Ecuador

E. Carrera Jarrin

Academy of Scientific Research and Technology of the Arab Republic of Egypt, Egyptian Network of High Energy Physics, Cairo, Egypt

Y. Assran^{8,9}, M.A. Mahmoud^{10,9}, A. Mahrous¹¹

National Institute of Chemical Physics and Biophysics, Tallinn, Estonia

R.K. Dewanjee, M. Kadastik, L. Perrini, M. Raidal, A. Tiko, C. Veelken

Department of Physics, University of Helsinki, Helsinki, Finland

P. Eerola, J. Pekkanen, M. Voutilainen

Helsinki Institute of Physics, Helsinki, Finland

J. Härkönen, T. Järvinen, V. Karimäki, R. Kinnunen, T. Lampén, K. Lassila-Perini, S. Lehti, T. Lindén, P. Luukka, E. Tuominen, J. Tuominiemi, E. Tuovinen

Lappeenranta University of Technology, Lappeenranta, Finland

J. Talvitie, T. Tuuva

IRFU, CEA, Université Paris-Saclay, Gif-sur-Yvette, France

M. Besancon, F. Couderc, M. Dejardin, D. Denegri, J.L. Faure, F. Ferri, S. Ganjour, S. Ghosh, A. Givernaud, P. Gras, G. Hamel de Monchenault, P. Jarry, I. Kucher, E. Locci, M. Mached, J. Malcles, G. Negro, J. Rander, A. Rosowsky, M.Ö. Sahin, M. Titov

Laboratoire Leprince-Ringuet, Ecole polytechnique, CNRS/IN2P3, Université Paris-Saclay, Palaiseau, France

A. Abdulsalam, I. Antropov, S. Baffioni, F. Beaudette, P. Busson, L. Cadamuro, C. Charlot, R. Granier de Cassagnac, M. Jo, S. Lisniak, A. Lobanov, J. Martin Blanco, M. Nguyen, C. Ochando, G. Ortona, P. Paganini, P. Pigard, S. Regnard, R. Salerno, J.B. Sauvan, Y. Sirois, A.G. Stahl Leiton, T. Strebler, Y. Yilmaz, A. Zabi

Université de Strasbourg, CNRS, IPHC UMR 7178, F-67000 Strasbourg, FranceJ.-L. Agram¹², J. Andrea, D. Bloch, J.-M. Brom, M. Buttignol, E.C. Chabert, N. Chanon, C. Collard, E. Conte¹², X. Coubez, J.-C. Fontaine¹², D. Gelé, U. Goerlach, M. Jansová, A.-C. Le Bihan, N. Tonon, P. Van Hove**Centre de Calcul de l'Institut National de Physique Nucleaire et de Physique des Particules, CNRS/IN2P3, Villeurbanne, France**

S. Gadrat

Université de Lyon, Université Claude Bernard Lyon 1, CNRS-IN2P3, Institut de Physique Nucléaire de Lyon, Villeurbanne, FranceS. Beauceron, C. Bernet, G. Boudoul, R. Chierici, D. Contardo, P. Depasse, H. El Mamouni, J. Fay, L. Finco, S. Gascon, M. Gouzevitch, G. Grenier, B. Ille, F. Lagarde, I.B. Laktineh, M. Lethuillier, L. Mirabito, A.L. Pequegnot, S. Perries, A. Popov¹³, V. Sordini, M. Vander Donckt, S. Viret**Georgian Technical University, Tbilisi, Georgia**T. Toriashvili¹⁴**Tbilisi State University, Tbilisi, Georgia**Z. Tsamalaidze⁷**RWTH Aachen University, I. Physikalisches Institut, Aachen, Germany**

C. Autermann, S. Beranek, L. Feld, M.K. Kiesel, K. Klein, M. Lipinski, M. Preuten, C. Schomakers, J. Schulz, T. Verlage

RWTH Aachen University, III. Physikalisches Institut A, Aachen, Germany

A. Albert, E. Dietz-Laursonn, D. Duchardt, M. Endres, M. Erdmann, S. Erdweg, T. Esch, R. Fischer, A. Güth, M. Hamer, T. Hebbeker, C. Heidemann, K. Hoepfner, S. Knutzen, M. Merschmeyer, A. Meyer, P. Millet, S. Mukherjee, M. Olschewski, K. Padeken, T. Pook, M. Radziej, H. Reithler, M. Rieger, F. Scheuch, D. Teyssier, S. Thüer

RWTH Aachen University, III. Physikalisches Institut B, Aachen, GermanyG. Flügge, B. Kargoll, T. Kress, A. Künsken, J. Lingemann, T. Müller, A. Nehr Korn, A. Nowack, C. Pistone, O. Pooth, A. Stahl¹⁵**Deutsches Elektronen-Synchrotron, Hamburg, Germany**M. Aldaya Martin, T. Arndt, C. Asawatangtrakuldee, K. Beernaert, O. Behnke, U. Behrens, A. Bermúdez Martínez, A.A. Bin Anuar, K. Borras¹⁶, V. Botta, A. Campbell, P. Connor, C. Contreras-Campana, F. Costanza, C. Diez Pardos, G. Eckerlin, D. Eckstein, T. Eichhorn,

E. Eren, E. Gallo¹⁷, J. Garay Garcia, A. Geiser, A. Gizhko, J.M. Grados Luyando, A. Grohsjean, P. Gunnellini, A. Harb, J. Hauk, M. Hempel¹⁸, H. Jung, A. Kalogeropoulos, M. Kasemann, J. Keaveney, C. Kleinwort, I. Korol, D. Krücker, W. Lange, A. Lelek, T. Lenz, J. Leonard, K. Lipka, W. Lohmann¹⁸, R. Mankel, I.-A. Melzer-Pellmann, A.B. Meyer, G. Mittag, J. Mnich, A. Mussgiller, E. Ntomari, D. Pitzl, R. Placakyte, A. Raspereza, B. Roland, M. Savitskyi, P. Saxena, R. Shevchenko, S. Spannagel, N. Stefaniuk, G.P. Van Onsem, R. Walsh, Y. Wen, K. Wichmann, C. Wissing, O. Zenaiev

University of Hamburg, Hamburg, Germany

S. Bein, V. Blobel, M. Centis Vignali, A.R. Draeger, T. Dreyer, E. Garutti, D. Gonzalez, J. Haller, A. Hinzmann, M. Hoffmann, A. Karavdina, R. Klanner, R. Kogler, N. Kovalchuk, S. Kurz, T. Lapsien, I. Marchesini, D. Marconi, M. Meyer, M. Niedziela, D. Nowatschin, F. Pantaleo¹⁵, T. Peiffer, A. Perieanu, C. Scharf, P. Schleper, A. Schmidt, S. Schumann, J. Schwandt, J. Sonneveld, H. Stadie, G. Steinbrück, F.M. Stober, M. Stöver, H. Tholen, D. Troendle, E. Usai, L. Vanelderen, A. Vanhoefer, B. Vormwald

Institut für Experimentelle Kernphysik, Karlsruhe, Germany

M. Akbiyik, C. Barth, S. Baur, E. Butz, R. Caspart, T. Chwalek, F. Colombo, W. De Boer, A. Dierlamm, B. Freund, R. Friese, M. Giffels, A. Gilbert, D. Haitz, F. Hartmann¹⁵, S.M. Heindl, U. Husemann, F. Kassel¹⁵, S. Kudella, H. Mildner, M.U. Mozer, Th. Müller, M. Plagge, G. Quast, K. Rabbertz, M. Schröder, I. Shvetsov, G. Sieber, H.J. Simonis, R. Ulrich, S. Wayand, M. Weber, T. Weiler, S. Williamson, C. Wöhrmann, R. Wolf

Institute of Nuclear and Particle Physics (INPP), NCSR Demokritos, Aghia Paraskevi, Greece

G. Anagnostou, G. Daskalakis, T. Gerasis, V.A. Giakoumopoulou, A. Kyriakis, D. Loukas, I. Topsis-Giotis

National and Kapodistrian University of Athens, Athens, Greece

S. Kesisoglou, A. Panagiotou, N. Saoulidou

University of Ioánnina, Ioánnina, Greece

I. Evangelou, C. Foudas, P. Kokkas, S. Mallios, N. Manthos, I. Papadopoulos, E. Paradas, J. Strologas, F.A. Triantis

MTA-ELTE Lendület CMS Particle and Nuclear Physics Group, Eötvös Loránd University, Budapest, Hungary

M. Csanad, N. Filipovic, G. Pasztor

Wigner Research Centre for Physics, Budapest, Hungary

G. Bencze, C. Hajdu, D. Horvath¹⁹, Á. Hunyadi, F. Sikler, V. Veszpremi, G. Vesztergombi²⁰, A.J. Zsigmond

Institute of Nuclear Research ATOMKI, Debrecen, Hungary

N. Beni, S. Czellar, J. Karancsi²¹, A. Makovec, J. Molnar, Z. Szillasi

Institute of Physics, University of Debrecen, Debrecen, Hungary

M. Bartók²⁰, P. Raics, Z.L. Trocsanyi, B. Ujvari

Indian Institute of Science (IISc), Bangalore, India

S. Choudhury, J.R. Komaragiri

National Institute of Science Education and Research, Bhubaneswar, India

S. Bahinipati²², S. Bhowmik, P. Mal, K. Mandal, A. Nayak²³, D.K. Sahoo²², N. Sahoo, S.K. Swain

Panjab University, Chandigarh, India

S. Bansal, S.B. Beri, V. Bhatnagar, U. Bhawandeep, R. Chawla, N. Dhingra, A.K. Kalsi, A. Kaur, M. Kaur, R. Kumar, P. Kumari, A. Mehta, J.B. Singh, G. Walia

University of Delhi, Delhi, India

Ashok Kumar, Aashaq Shah, A. Bhardwaj, S. Chauhan, B.C. Choudhary, R.B. Garg, S. Keshri, A. Kumar, S. Malhotra, M. Naimuddin, K. Ranjan, R. Sharma, V. Sharma

Saha Institute of Nuclear Physics, HBNI, Kolkata, India

R. Bhardwaj, R. Bhattacharya, S. Bhattacharya, S. Dey, S. Dutt, S. Dutta, S. Ghosh, N. Majumdar, A. Modak, K. Mondal, S. Mukhopadhyay, S. Nandan, A. Purohit, A. Roy, D. Roy, S. Roy Chowdhury, S. Sarkar, M. Sharan, S. Thakur

Indian Institute of Technology Madras, Madras, India

P.K. Behera

Bhabha Atomic Research Centre, Mumbai, India

R. Chudasama, D. Dutta, V. Jha, V. Kumar, A.K. Mohanty¹⁵, P.K. Netrakanti, L.M. Pant, P. Shukla, A. Topkar

Tata Institute of Fundamental Research-A, Mumbai, India

T. Aziz, S. Dugad, B. Mahakud, S. Mitra, G.B. Mohanty, B. Parida, N. Sur, B. Sutar

Tata Institute of Fundamental Research-B, Mumbai, India

S. Banerjee, S. Bhattacharya, S. Chatterjee, P. Das, M. Guchait, Sa. Jain, S. Kumar, M. Maity²⁴, G. Majumder, K. Mazumdar, T. Sarkar²⁴, N. Wickramage²⁵

Indian Institute of Science Education and Research (IISER), Pune, India

S. Chauhan, S. Dube, V. Hegde, A. Kapoor, K. Kotheekar, S. Pandey, A. Rane, S. Sharma

Institute for Research in Fundamental Sciences (IPM), Tehran, Iran

S. Chenarani²⁶, E. Eskandari Tadavani, S.M. Etesami²⁶, M. Khakzad, M. Mohammadi Najafabadi, M. Naseri, S. Paktinat Mehdiabadi²⁷, F. Rezaei Hosseinabadi, B. Safarzadeh²⁸, M. Zeinali

University College Dublin, Dublin, Ireland

M. Felcini, M. Grunewald

INFN Sezione di Bari ^a, Università di Bari ^b, Politecnico di Bari ^c, Bari, Italy

M. Abbrescia^{a,b}, C. Calabria^{a,b}, C. Caputo^{a,b}, A. Colaleo^a, D. Creanza^{a,c}, L. Cristella^{a,b}, N. De Filippis^{a,c}, M. De Palma^{a,b}, F. Errico^{a,b}, L. Fiore^a, G. Iaselli^{a,c}, S. Lezki^{a,b}, G. Maggi^{a,c}, M. Maggi^a, G. Miniello^{a,b}, S. My^{a,b}, S. Nuzzo^{a,b}, A. Pompili^{a,b}, G. Pugliese^{a,c}, R. Radogna^{a,b}, A. Ranieri^a, G. Selvaggi^{a,b}, A. Sharma^a, L. Silvestris^{a,15}, R. Venditti^a, P. Verwilligen^a

INFN Sezione di Bologna ^a, Università di Bologna ^b, Bologna, Italy

G. Abbiendi^a, C. Battilana^{a,b}, D. Bonacorsi^{a,b}, S. Braibant-Giacomelli^{a,b}, R. Campanini^{a,b}, P. Capiluppi^{a,b}, A. Castro^{a,b}, F.R. Cavallo^a, S.S. Chhibra^a, G. Codispoti^{a,b}, M. Cuffiani^{a,b}, G.M. Dallavalle^a, F. Fabbri^a, A. Fanfani^{a,b}, D. Fasanella^{a,b}, P. Giacomelli^a, C. Grandi^a, L. Guiducci^{a,b}, S. Marcellini^a, G. Masetti^a, A. Montanari^a, F.L. Navarra^{a,b}, A. Perrotta^a, A.M. Rossi^{a,b}, T. Rovelli^{a,b}, G.P. Siroli^{a,b}, N. Tosi^a

INFN Sezione di Catania ^a, Università di Catania ^b, Catania, Italy

S. Albergo^{a,b}, S. Costa^{a,b}, A. Di Mattia^a, F. Giordano^{a,b}, R. Potenza^{a,b}, A. Tricomi^{a,b}, C. Tuve^{a,b}

INFN Sezione di Firenze ^a, Università di Firenze ^b, Firenze, Italy

G. Barbagli^a, K. Chatterjee^{a,b}, V. Ciulli^{a,b}, C. Civinini^a, R. D'Alessandro^{a,b}, E. Focardi^{a,b}, P. Lenzi^{a,b}, M. Meschini^a, S. Paoletti^a, L. Russo^{a,29}, G. Sguazzoni^a, D. Strom^a, L. Viliani^{a,b,15}

INFN Laboratori Nazionali di Frascati, Frascati, Italy

L. Benussi, S. Bianco, F. Fabbri, D. Piccolo, F. Primavera¹⁵

INFN Sezione di Genova ^a, Università di Genova ^b, Genova, Italy

V. Calvelli^{a,b}, F. Ferro^a, E. Robutti^a, S. Tosi^{a,b}

INFN Sezione di Milano-Bicocca ^a, Università di Milano-Bicocca ^b, Milano, Italy

L. Brianza^{a,b}, F. Brivio^{a,b}, V. Ciriolo^{a,b}, M.E. Dinardo^{a,b}, S. Fiorendi^{a,b}, S. Gennai^a, A. Ghezzi^{a,b}, P. Govoni^{a,b}, M. Malberti^{a,b}, S. Malvezzi^a, R.A. Manzoni^{a,b}, D. Menasce^a, L. Moroni^a, M. Paganoni^{a,b}, K. Pauwels^{a,b}, D. Pedrini^a, S. Pigazzini^{a,b,30}, S. Ragazzi^{a,b}, T. Tabarelli de Fatis^{a,b}

INFN Sezione di Napoli ^a, Università di Napoli 'Federico II' ^b, Napoli, Italy, Università della Basilicata ^c, Potenza, Italy, Università G. Marconi ^d, Roma, Italy

S. Buontempo^a, N. Cavallo^{a,c}, S. Di Guida^{a,d,15}, M. Esposito^{a,b}, F. Fabozzi^{a,c}, F. Fienga^{a,b}, A.O.M. Iorio^{a,b}, W.A. Khan^a, G. Lanza^a, L. Lista^a, S. Meola^{a,d,15}, P. Paolucci^{a,15}, C. Sciacca^{a,b}, F. Thyssen^a

INFN Sezione di Padova ^a, Università di Padova ^b, Padova, Italy, Università di Trento ^c, Trento, Italy

P. Azzi^{a,15}, S. Badoer^a, M. Bellato^a, L. Benato^{a,b}, M. Benettoni^a, D. Bisello^{a,b}, A. Boletti^{a,b}, R. Carlin^{a,b}, A. Carvalho Antunes De Oliveira^{a,b}, M. Dall'Osso^{a,b}, P. De Castro Manzano^a, T. Dorigo^a, U. Dosselli^a, F. Gasparini^{a,b}, U. Gasparini^{a,b}, A. Gozzelino^a, S. Lacaprara^a, A.T. Meneguzzo^{a,b}, N. Pozzobon^{a,b}, P. Ronchese^{a,b}, R. Rossin^{a,b}, F. Simonetto^{a,b}, E. Torassa^a, M. Zanetti^{a,b}, P. Zotto^{a,b}, G. Zumerle^{a,b}

INFN Sezione di Pavia ^a, Università di Pavia ^b, Pavia, Italy

A. Braghieri^a, F. Fallavollita^{a,b}, A. Magnani^{a,b}, P. Montagna^{a,b}, S.P. Ratti^{a,b}, V. Re^a, M. Ressegotti, C. Riccardi^{a,b}, P. Salvini^a, I. Vai^{a,b}, P. Vitulo^{a,b}

INFN Sezione di Perugia ^a, Università di Perugia ^b, Perugia, Italy

L. Alunni Solestizi^{a,b}, M. Biasini^{a,b}, G.M. Bilei^a, C. Cecchi^{a,b}, D. Ciangottini^{a,b}, L. Fanò^{a,b}, P. Lariccia^{a,b}, R. Leonardi^{a,b}, E. Manoni^a, G. Mantovani^{a,b}, V. Mariani^{a,b}, M. Menichelli^a, A. Rossi^{a,b}, A. Santocchia^{a,b}, D. Spiga^a

INFN Sezione di Pisa ^a, Università di Pisa ^b, Scuola Normale Superiore di Pisa ^c, Pisa, Italy

K. Androsov^a, P. Azzurri^{a,15}, G. Bagliesi^a, J. Bernardini^a, T. Boccali^a, L. Borrello, R. Castaldi^a, M.A. Ciocci^{a,b}, R. Dell'Orso^a, G. Fedi^a, L. Giannini^{a,c}, A. Giassi^a, M.T. Grippo^{a,29}, F. Ligabue^{a,c}, T. Lomtadze^a, E. Manca^{a,c}, G. Mandorli^{a,c}, L. Martini^{a,b}, A. Messineo^{a,b}, F. Palla^a, A. Rizzi^{a,b}, A. Savoy-Navarro^{a,31}, P. Spagnolo^a, R. Tenchini^a, G. Tonelli^{a,b}, A. Venturi^a, P.G. Verdini^a

INFN Sezione di Roma ^a, Sapienza Università di Roma ^b, Rome, Italy

L. Barone^{a,b}, F. Cavallari^a, M. Cipriani^{a,b}, D. Del Re^{a,b,15}, M. Diemoz^a, S. Gelli^{a,b}, E. Longo^{a,b}, F. Margaroli^{a,b}, B. Marzocchi^{a,b}, P. Meridiani^a, G. Organtini^{a,b}, R. Paramatti^{a,b}, F. Preiato^{a,b}, S. Rahatlou^{a,b}, C. Rovelli^a, F. Santanastasio^{a,b}

INFN Sezione di Torino ^a, Università di Torino ^b, Torino, Italy, Università del Piemonte Orientale ^c, Novara, Italy

N. Amapane^{a,b}, R. Arcidiacono^{a,c}, S. Argiro^{a,b}, M. Arneodo^{a,c}, N. Bartosik^a, R. Bellan^{a,b}, C. Biino^a, N. Cartiglia^a, F. Cenna^{a,b}, M. Costa^{a,b}, R. Covarelli^{a,b}, A. Degano^{a,b}, N. Demaria^a

B. Kiani^{a,b}, C. Mariotti^a, S. Maselli^a, E. Migliore^{a,b}, V. Monaco^{a,b}, E. Monteil^{a,b}, M. Monteno^a, M.M. Obertino^{a,b}, L. Pacher^{a,b}, N. Pastrone^a, M. Pelliccioni^a, G.L. Pinna Angioni^{a,b}, F. Ravera^{a,b}, A. Romero^{a,b}, M. Ruspa^{a,c}, R. Sacchi^{a,b}, K. Shchelina^{a,b}, V. Sola^a, A. Solano^{a,b}, A. Staiano^a, P. Traczyk^{a,b}

INFN Sezione di Trieste ^a, Università di Trieste ^b, Trieste, Italy

S. Belforte^a, M. Casarsa^a, F. Cossutti^a, G. Della Ricca^{a,b}, A. Zanetti^a

Kyungpook National University, Daegu, Korea

D.H. Kim, G.N. Kim, M.S. Kim, J. Lee, S. Lee, S.W. Lee, C.S. Moon, Y.D. Oh, S. Sekmen, D.C. Son, Y.C. Yang

Chonbuk National University, Jeonju, Korea

A. Lee

Chonnam National University, Institute for Universe and Elementary Particles, Kwangju, Korea

H. Kim, D.H. Moon, G. Oh

Hanyang University, Seoul, Korea

J.A. Brochero Cifuentes, J. Goh, T.J. Kim

Korea University, Seoul, Korea

S. Cho, S. Choi, Y. Go, D. Gyun, S. Ha, B. Hong, Y. Jo, Y. Kim, K. Lee, K.S. Lee, S. Lee, J. Lim, S.K. Park, Y. Roh

Seoul National University, Seoul, Korea

J. Almond, J. Kim, J.S. Kim, H. Lee, K. Lee, K. Nam, S.B. Oh, B.C. Radburn-Smith, S.h. Seo, U.K. Yang, H.D. Yoo, G.B. Yu

University of Seoul, Seoul, Korea

M. Choi, H. Kim, J.H. Kim, J.S.H. Lee, I.C. Park, G. Ryu

Sungkyunkwan University, Suwon, Korea

Y. Choi, C. Hwang, J. Lee, I. Yu

Vilnius University, Vilnius, Lithuania

V. Dudenas, A. Juodagalvis, J. Vaitkus

National Centre for Particle Physics, Universiti Malaya, Kuala Lumpur, Malaysia

I. Ahmed, Z.A. Ibrahim, M.A.B. Md Ali³², F. Mohamad Idris³³, W.A.T. Wan Abdullah, M.N. Yusli, Z. Zolkapli

Centro de Investigacion y de Estudios Avanzados del IPN, Mexico City, Mexico

H. Castilla-Valdez, E. De La Cruz-Burelo, I. Heredia-De La Cruz³⁴, R. Lopez-Fernandez, J. Mejia Guisao, A. Sanchez-Hernandez

Universidad Iberoamericana, Mexico City, Mexico

S. Carrillo Moreno, C. Oropeza Barrera, F. Vazquez Valencia

Benemerita Universidad Autonoma de Puebla, Puebla, Mexico

I. Pedraza, H.A. Salazar Ibarguen, C. Uribe Estrada

Universidad Autónoma de San Luis Potosí, San Luis Potosí, Mexico

A. Morelos Pineda

University of Auckland, Auckland, New Zealand

D. Krofcheck

University of Canterbury, Christchurch, New Zealand

P.H. Butler

National Centre for Physics, Quaid-I-Azam University, Islamabad, Pakistan

A. Ahmad, M. Ahmad, Q. Hassan, H.R. Hoorani, A. Saddique, M.A. Shah, M. Shoaib, M. Waqas

National Centre for Nuclear Research, Swierk, Poland

H. Bialkowska, M. Bluj, B. Boimska, T. Frueboes, M. Górski, M. Kazana, K. Nawrocki, K. Romanowska-Rybinska, M. Szleper, P. Zalewski

Institute of Experimental Physics, Faculty of Physics, University of Warsaw, Warsaw, PolandK. Bunkowski, A. Byszuk³⁵, K. Doroba, A. Kalinowski, M. Konecki, J. Krolikowski, M. Misiura, M. Olszewski, A. Pyskir, M. Walczak**Laboratório de Instrumentação e Física Experimental de Partículas, Lisboa, Portugal**

P. Bargassa, C. Beirão Da Cruz E Silva, B. Calpas, A. Di Francesco, P. Faccioli, M. Gallinaro, J. Hollar, N. Leonardo, L. Lloret Iglesias, M.V. Nemallapudi, J. Seixas, O. Toldaiev, D. Vadrucchio, J. Varela

Joint Institute for Nuclear Research, Dubna, RussiaS. Afanasiev, P. Bunin, M. Gavrilenko, I. Golutvin, I. Gorbunov, A. Kamenev, V. Karjavin, A. Lanev, A. Malakhov, V. Matveev^{36,37}, V. Palichik, V. Perelygin, S. Shmatov, S. Shulha, N. Skatchkov, V. Smirnov, N. Voytishin, A. Zarubin**Petersburg Nuclear Physics Institute, Gatchina (St. Petersburg), Russia**Y. Ivanov, V. Kim³⁸, E. Kuznetsova³⁹, P. Levchenko, V. Murzin, V. Oreshkin, I. Smirnov, V. Sulimov, L. Uvarov, S. Vavilov, A. Vorobyev**Institute for Nuclear Research, Moscow, Russia**

Yu. Andreev, A. Dermenev, S. Gninenko, N. Golubev, A. Karneyeu, M. Kirsanov, N. Krasnikov, A. Pashenkov, D. Tlisov, A. Toropin

Institute for Theoretical and Experimental Physics, Moscow, Russia

V. Epshteyn, V. Gavrilov, N. Lychkovskaya, V. Popov, I. Pozdnyakov, G. Safronov, A. Spiridonov, A. Stepenov, M. Toms, E. Vlasov, A. Zhokin

Moscow Institute of Physics and Technology, Moscow, RussiaT. Aushev, A. Bylinkin³⁷**National Research Nuclear University 'Moscow Engineering Physics Institute' (MEPhI), Moscow, Russia**M. Chadeeva⁴⁰, O. Markin, P. Parygin, D. Philippov, S. Polikarpov, V. Rusinov**P.N. Lebedev Physical Institute, Moscow, Russia**V. Andreev, M. Azarkin³⁷, I. Dremin³⁷, M. Kirakosyan³⁷, A. Terkulov**Skobeltsyn Institute of Nuclear Physics, Lomonosov Moscow State University, Moscow, Russia**A. Baskakov, A. Belyaev, E. Boos, V. Bunichev, M. Dubinin⁴¹, L. Dudko, A. Ershov, A. Gribushin, V. Klyukhin, O. Kodolova, I. Lokhtin, I. Miagkov, S. Obraztsov, S. Petrushanko, V. Savrin**Novosibirsk State University (NSU), Novosibirsk, Russia**V. Blinov⁴², Y. Skovpen⁴², D. Shtol⁴²

State Research Center of Russian Federation, Institute for High Energy Physics, Protvino, Russia

I. Azhgirey, I. Bayshev, S. Bitioukov, D. Elumakhov, V. Kachanov, A. Kalinin, D. Konstantinov, V. Krychkin, V. Petrov, R. Ryutin, A. Sobol, S. Troshin, N. Tyurin, A. Uzunian, A. Volkov

University of Belgrade, Faculty of Physics and Vinca Institute of Nuclear Sciences, Belgrade, Serbia

P. Adzic⁴³, P. Cirkovic, D. Devetak, M. Dordevic, J. Milosevic, V. Rekovic

Centro de Investigaciones Energéticas Medioambientales y Tecnológicas (CIEMAT), Madrid, Spain

J. Alcaraz Maestre, M. Barrio Luna, M. Cerrada, N. Colino, B. De La Cruz, A. Delgado Peris, A. Escalante Del Valle, C. Fernandez Bedoya, J.P. Fernández Ramos, J. Flix, M.C. Fouz, P. Garcia-Abia, O. Gonzalez Lopez, S. Goy Lopez, J.M. Hernandez, M.I. Josa, A. Pérez-Calero Yzquierdo, J. Puerta Pelayo, A. Quintario Olmeda, I. Redondo, L. Romero, M.S. Soares, A. Álvarez Fernández

Universidad Autónoma de Madrid, Madrid, Spain

J.F. de Trocóniz, M. Missiroli, D. Moran

Universidad de Oviedo, Oviedo, Spain

J. Cuevas, C. Erice, J. Fernandez Menendez, I. Gonzalez Caballero, J.R. González Fernández, E. Palencia Cortezon, S. Sanchez Cruz, I. Suárez Andrés, P. Vischia, J.M. Vizán Garcia

Instituto de Física de Cantabria (IFCA), CSIC-Universidad de Cantabria, Santander, Spain

I.J. Cabrillo, A. Calderon, B. Chazin Quero, E. Curras, M. Fernandez, J. Garcia-Ferrero, G. Gomez, A. Lopez Virto, J. Marco, C. Martinez Rivero, P. Martinez Ruiz del Arbol, F. Matorras, J. Piedra Gomez, T. Rodrigo, A. Ruiz-Jimeno, L. Scodellaro, N. Trevisani, I. Vila, R. Vilar Cortabitarte

CERN, European Organization for Nuclear Research, Geneva, Switzerland

D. Abbaneo, E. Auffray, P. Baillon, A.H. Ball, D. Barney, M. Bianco, P. Bloch, A. Bocci, C. Botta, T. Camporesi, R. Castello, M. Cepeda, G. Cerminara, E. Chapon, Y. Chen, D. d'Enterria, A. Dabrowski, V. Daponte, A. David, M. De Gruttola, A. De Roeck, E. Di Marco⁴⁴, M. Dobson, B. Dorney, T. du Pree, M. Dünser, N. Dupont, A. Elliott-Peisert, P. Everaerts, G. Franzoni, J. Fulcher, W. Funk, D. Gigi, K. Gill, F. Glege, D. Gulhan, S. Gundacker, M. Guthoff, P. Harris, J. Hegeman, V. Innocente, P. Janot, O. Karacheban¹⁸, J. Kieseler, H. Kirschenmann, V. Knünz, A. Kornmayer¹⁵, M.J. Kortelainen, C. Lange, P. Lecoq, C. Lourenço, M.T. Lucchini, L. Malgeri, M. Mannelli, A. Martelli, F. Meijers, J.A. Merlin, S. Mersi, E. Meschi, P. Milenovic⁴⁵, F. Moortgat, M. Mulders, H. Neugebauer, S. Orfanelli, L. Orsini, L. Pape, E. Perez, M. Peruzzi, A. Petrilli, G. Petrucciani, A. Pfeiffer, M. Pierini, A. Racz, T. Reis, G. Rolandi⁴⁶, M. Rovere, H. Sakulin, C. Schäfer, C. Schwick, M. Seidel, M. Selvaggi, A. Sharma, P. Silva, P. Sphicas⁴⁷, J. Steggemann, M. Stoye, M. Tosi, D. Treille, A. Triossi, A. Tsirou, V. Veckalns⁴⁸, G.I. Veres²⁰, M. Verweij, N. Wardle, W.D. Zeuner

Paul Scherrer Institut, Villigen, Switzerland

W. Bertl[†], L. Caminada⁴⁹, K. Deiters, W. Erdmann, R. Horisberger, Q. Ingram, H.C. Kaestli, D. Kotlinski, U. Langenegger, T. Rohe, S.A. Wiederkehr

Institute for Particle Physics, ETH Zurich, Zurich, Switzerland

F. Bachmair, L. Bäni, P. Berger, L. Bianchini, B. Casal, G. Dissertori, M. Dittmar, M. Donegà, C. Grab, C. Heidegger, D. Hits, J. Hoss, G. Kasieczka, T. Klijsma, W. Lustermann, B. Mangano, M. Marionneau, M.T. Meinhard, D. Meister, F. Micheli, P. Musella, F. Nessi-Tedaldi, F. Pandolfi,

J. Pata, F. Pauss, G. Perrin, L. Perrozzi, M. Quittnat, M. Schönenberger, L. Shchutska, V.R. Tavolaro, K. Theofilatos, M.L. Vesterbacka Olsson, R. Wallny, A. Zagozdzińska³⁵, D.H. Zhu

Universität Zürich, Zurich, Switzerland

T.K. Aarrestad, C. AMSler⁵⁰, M.F. Canelli, A. De Cosa, S. Donato, C. Galloni, T. Hreus, B. Kilminster, J. Ngadiuba, D. Pinna, G. Rauco, P. Robmann, D. Salerno, C. Seitz, A. Zucchetta

National Central University, Chung-Li, Taiwan

V. Candelise, T.H. Doan, Sh. Jain, R. Khurana, C.M. Kuo, W. Lin, A. Pozdnyakov, S.S. Yu

National Taiwan University (NTU), Taipei, Taiwan

Arun Kumar, P. Chang, Y. Chao, K.F. Chen, P.H. Chen, F. Fiori, W.-S. Hou, Y. Hsiung, Y.F. Liu, R.-S. Lu, M. Miñano Moya, E. Paganis, A. Psallidas, J.f. Tsai

Chulalongkorn University, Faculty of Science, Department of Physics, Bangkok, Thailand

B. Asavapibhop, K. Kovitanggoon, G. Singh, N. Srimanobhas

ukurova University, Physics Department, Science and Art Faculty, Adana, Turkey

A. Adiguzel⁵¹, F. Boran, S. Damarseekin, Z.S. Demiroglu, C. Dozen, E. Eskut, S. Girgis, G. Gokbulut, Y. Guler, I. Hos⁵², E.E. Kangal⁵³, O. Kara, A. Kayis Topaksu, U. Kiminsu, M. Oglakci, G. Onengut⁵⁴, K. Ozdemir⁵⁵, S. Ozturk⁵⁶, A. Polatoz, B. Tali⁵⁷, S. Turkcapar, I.S. Zorbakir, C. Zorbilmez

Middle East Technical University, Physics Department, Ankara, Turkey

B. Bilin, G. Karapinar⁵⁸, K. Ocalan⁵⁹, M. Yalvac, M. Zeyrek

Bogazici University, Istanbul, Turkey

E. Gülmez, M. Kaya⁶⁰, O. Kaya⁶¹, S. Tekten, E.A. Yetkin⁶²

Istanbul Technical University, Istanbul, Turkey

M.N. Agaras, S. Atay, A. Cakir, K. Cankocak

Institute for Scintillation Materials of National Academy of Science of Ukraine, Kharkov, Ukraine

B. Grynyov

National Scientific Center, Kharkov Institute of Physics and Technology, Kharkov, Ukraine

L. Levchuk, P. Sorokin

University of Bristol, Bristol, United Kingdom

R. Aggleton, F. Ball, L. Beck, J.J. Brooke, D. Burns, E. Clement, D. Cussans, O. Davignon, H. Flacher, J. Goldstein, M. Grimes, G.P. Heath, H.F. Heath, J. Jacob, L. Kreczko, C. Lucas, D.M. Newbold⁶³, S. Paramesvaran, A. Poll, T. Sakuma, S. Seif El Nasr-storey, D. Smith, V.J. Smith

Rutherford Appleton Laboratory, Didcot, United Kingdom

K.W. Bell, A. Belyaev⁶⁴, C. Brew, R.M. Brown, L. Calligaris, D. Cieri, D.J.A. Cockerill, J.A. Coughlan, K. Harder, S. Harper, J. Linacre, E. Olaiya, D. Petyt, C.H. Shepherd-Themistocleous, A. Thea, I.R. Tomalin, T. Williams

Imperial College, London, United Kingdom

R. Bainbridge, S. Breeze, O. Buchmuller, A. Bundock, S. Casasso, M. Citron, D. Colling, L. Corpe, P. Dauncey, G. Davies, A. De Wit, M. Della Negra, R. Di Maria, A. Elwood, Y. Haddad, G. Hall, G. Iles, T. James, R. Lane, C. Laner, L. Lyons, A.-M. Magnan, S. Malik, L. Mastrolorenzo, T. Matsushita, J. Nash, A. Nikitenko⁶, V. Palladino, M. Pesaresi, D.M. Raymond, A. Richards,

A. Rose, E. Scott, C. Seez, A. Shtipliyski, S. Summers, A. Tapper, K. Uchida, M. Vazquez Acosta⁶⁵, T. Virdee¹⁵, D. Winterbottom, J. Wright, S.C. Zenz

Brunel University, Uxbridge, United Kingdom

J.E. Cole, P.R. Hobson, A. Khan, P. Kyberd, I.D. Reid, P. Symonds, L. Teodorescu, M. Turner

Baylor University, Waco, USA

A. Borzou, K. Call, J. Dittmann, K. Hatakeyama, H. Liu, N. Pastika, C. Smith

Catholic University of America, Washington DC, USA

R. Bartek, A. Dominguez

The University of Alabama, Tuscaloosa, USA

A. Buccilli, S.I. Cooper, C. Henderson, P. Rumerio, C. West

Boston University, Boston, USA

D. Arcaro, A. Avetisyan, T. Bose, D. Gastler, D. Rankin, C. Richardson, J. Rohlf, L. Sulak, D. Zou

Brown University, Providence, USA

G. Benelli, D. Cutts, A. Garabedian, J. Hakala, U. Heintz, J.M. Hogan, K.H.M. Kwok, E. Laird, G. Landsberg, Z. Mao, M. Narain, S. Piperov, S. Sagir, R. Syarif

University of California, Davis, Davis, USA

R. Band, C. Brainerd, D. Burns, M. Calderon De La Barca Sanchez, M. Chertok, J. Conway, R. Conway, P.T. Cox, R. Erbacher, C. Flores, G. Funk, M. Gardner, W. Ko, R. Lander, C. Mclean, M. Mulhearn, D. Pellett, J. Pilot, S. Shalhout, M. Shi, J. Smith, M. Squires, D. Stolp, K. Tos, M. Tripathi, Z. Wang

University of California, Los Angeles, USA

M. Bachtis, C. Bravo, R. Cousins, A. Dasgupta, A. Florent, J. Hauser, M. Ignatenko, N. Mccoll, D. Saltzberg, C. Schnaible, V. Valuev

University of California, Riverside, Riverside, USA

E. Bouvier, K. Burt, R. Clare, J. Ellison, J.W. Gary, S.M.A. Ghiasi Shirazi, G. Hanson, J. Heilman, P. Jandir, E. Kennedy, F. Lacroix, O.R. Long, M. Olmedo Negrete, M.I. Paneva, A. Shrinivas, W. Si, L. Wang, H. Wei, S. Wimpenny, B. R. Yates

University of California, San Diego, La Jolla, USA

J.G. Branson, S. Cittolin, M. Derdzinski, B. Hashemi, A. Holzner, D. Klein, G. Kole, V. Krutelyov, J. Letts, I. Macneill, M. Masciovecchio, D. Olivito, S. Padhi, M. Pieri, M. Sani, V. Sharma, S. Simon, M. Tadel, A. Vartak, S. Wasserbaech⁶⁶, J. Wood, F. Würthwein, A. Yagil, G. Zevi Della Porta

University of California, Santa Barbara - Department of Physics, Santa Barbara, USA

N. Amin, R. Bhandari, J. Bradmiller-Feld, C. Campagnari, A. Dishaw, V. Dutta, M. Franco Sevilla, C. George, F. Golf, L. Gouskos, J. Gran, R. Heller, J. Incandela, S.D. Mullin, A. Ovcharova, H. Qu, J. Richman, D. Stuart, I. Suarez, J. Yoo

California Institute of Technology, Pasadena, USA

D. Anderson, J. Bendavid, A. Bornheim, J.M. Lawhorn, H.B. Newman, T. Nguyen, C. Pena, M. Spiropulu, J.R. Vlimant, S. Xie, Z. Zhang, R.Y. Zhu

Carnegie Mellon University, Pittsburgh, USA

M.B. Andrews, T. Ferguson, T. Mudholkar, M. Paulini, J. Russ, M. Sun, H. Vogel, I. Vorobiev, M. Weinberg

University of Colorado Boulder, Boulder, USA

J.P. Cumalat, W.T. Ford, F. Jensen, A. Johnson, M. Krohn, S. Leontsinis, T. Mulholland, K. Stenson, S.R. Wagner

Cornell University, Ithaca, USA

J. Alexander, J. Chaves, J. Chu, S. Dittmer, K. Mcdermott, N. Mirman, J.R. Patterson, A. Rinkevicius, A. Ryd, L. Skinnari, L. Soffi, S.M. Tan, Z. Tao, J. Thom, J. Tucker, P. Wittich, M. Zientek

Fermi National Accelerator Laboratory, Batavia, USA

S. Abdullin, M. Albrow, G. Apollinari, A. Apresyan, A. Apyan, S. Banerjee, L.A.T. Bauerdick, A. Beretvas, J. Berryhill, P.C. Bhat, G. Bolla, K. Burkett, J.N. Butler, A. Canepa, G.B. Cerati, H.W.K. Cheung, F. Chlebana, M. Cremonesi, J. Duarte, V.D. Elvira, J. Freeman, Z. Gecse, E. Gottschalk, L. Gray, D. Green, S. Grünendahl, O. Gutsche, R.M. Harris, S. Hasegawa, J. Hirschauer, Z. Hu, B. Jayatilaka, S. Jindariani, M. Johnson, U. Joshi, B. Klima, B. Kreis, S. Lammel, D. Lincoln, R. Lipton, M. Liu, T. Liu, R. Lopes De Sá, J. Lykken, K. Maeshima, N. Magini, J.M. Marraffino, S. Maruyama, D. Mason, P. McBride, P. Merkel, S. Mrenna, S. Nahn, V. O'Dell, K. Pedro, O. Prokofyev, G. Rakness, L. Ristori, B. Schneider, E. Sexton-Kennedy, A. Soha, W.J. Spalding, L. Spiegel, S. Stoynev, J. Strait, N. Strobbe, L. Taylor, S. Tkaczyk, N.V. Tran, L. Uplegger, E.W. Vaandering, C. Vernieri, M. Verzocchi, R. Vidal, M. Wang, H.A. Weber, A. Whitbeck

University of Florida, Gainesville, USA

D. Acosta, P. Avery, P. Bortignon, D. Bourilkov, A. Brinkerhoff, A. Carnes, M. Carver, D. Curry, S. Das, R.D. Field, I.K. Furic, J. Konigsberg, A. Korytov, K. Kotov, P. Ma, K. Matchev, H. Mei, G. Mitselmakher, D. Rank, D. Sperka, N. Terentyev, L. Thomas, J. Wang, S. Wang, J. Yelton

Florida International University, Miami, USA

Y.R. Joshi, S. Linn, P. Markowitz, J.L. Rodriguez

Florida State University, Tallahassee, USA

A. Ackert, T. Adams, A. Askew, S. Hagopian, V. Hagopian, K.F. Johnson, T. Kolberg, G. Martinez, T. Perry, H. Prosper, A. Saha, A. Santra, R. Yohay

Florida Institute of Technology, Melbourne, USA

M.M. Baarmand, V. Bhopatkar, S. Colafranceschi, M. Hohlmann, D. Noonan, T. Roy, F. Yumiceva

University of Illinois at Chicago (UIC), Chicago, USA

M.R. Adams, L. Apanasevich, D. Berry, R.R. Betts, R. Cavanaugh, X. Chen, O. Evdokimov, C.E. Gerber, D.A. Hangal, D.J. Hofman, K. Jung, J. Kamin, I.D. Sandoval Gonzalez, M.B. Tonjes, H. Trauger, N. Varelas, H. Wang, Z. Wu, J. Zhang

The University of Iowa, Iowa City, USA

B. Bilki⁶⁷, W. Clarida, K. Dilsiz⁶⁸, S. Durgut, R.P. Gandrajula, M. Haytmyradov, V. Khristenko, J.-P. Merlo, H. Mermerkaya⁶⁹, A. Mestvirishvili, A. Moeller, J. Nachtman, H. Ogul⁷⁰, Y. Onel, F. Ozok⁷¹, A. Penzo, C. Snyder, E. Tiras, J. Wetzel, K. Yi

Johns Hopkins University, Baltimore, USA

B. Blumenfeld, A. Cocoros, N. Eminizer, D. Fehling, L. Feng, A.V. Gritsan, P. Maksimovic, J. Roskes, U. Sarica, M. Swartz, M. Xiao, C. You

The University of Kansas, Lawrence, USA

A. Al-bataineh, P. Baringer, A. Bean, S. Boren, J. Bowen, J. Castle, S. Khalil, A. Kropivnitskaya,

D. Majumder, W. Mcbrayer, M. Murray, C. Royon, S. Sanders, E. Schmitz, R. Stringer, J.D. Tapia Takaki, Q. Wang

Kansas State University, Manhattan, USA

A. Ivanov, K. Kaadze, Y. Maravin, A. Mohammadi, L.K. Saini, N. Skhirtladze, S. Toda

Lawrence Livermore National Laboratory, Livermore, USA

F. Rebassoo, D. Wright

University of Maryland, College Park, USA

C. Anelli, A. Baden, O. Baron, A. Belloni, B. Calvert, S.C. Eno, C. Ferraioli, N.J. Hadley, S. Jabeen, G.Y. Jeng, R.G. Kellogg, J. Kunkle, A.C. Mignerey, F. Ricci-Tam, Y.H. Shin, A. Skuja, S.C. Tonwar

Massachusetts Institute of Technology, Cambridge, USA

D. Abercrombie, B. Allen, V. Azzolini, R. Barbieri, A. Baty, R. Bi, S. Brandt, W. Busza, I.A. Cali, M. D'Alfonso, Z. Demiragli, G. Gomez Ceballos, M. Goncharov, D. Hsu, Y. Iiyama, G.M. Innocenti, M. Klute, D. Kovalskyi, Y.S. Lai, Y.-J. Lee, A. Levin, P.D. Luckey, B. Maier, A.C. Marini, C. Mcginn, C. Mironov, S. Narayanan, X. Niu, C. Paus, C. Roland, G. Roland, J. Salfeld-Nebgen, G.S.F. Stephans, K. Tatar, D. Velicanu, J. Wang, T.W. Wang, B. Wyslouch

University of Minnesota, Minneapolis, USA

A.C. Benvenuti, R.M. Chatterjee, A. Evans, P. Hansen, S. Kalafut, Y. Kubota, Z. Lesko, J. Mans, S. Nourbakhsh, N. Ruckstuhl, R. Rusack, J. Turkewitz

University of Mississippi, Oxford, USA

J.G. Acosta, S. Oliveros

University of Nebraska-Lincoln, Lincoln, USA

E. Avdeeva, K. Bloom, D.R. Claes, C. Fangmeier, R. Gonzalez Suarez, R. Kamalieddin, I. Kravchenko, J. Monroy, J.E. Siado, G.R. Snow, B. Stieger

State University of New York at Buffalo, Buffalo, USA

M. Alyari, J. Dolen, A. Godshalk, C. Harrington, I. Iashvili, D. Nguyen, A. Parker, S. Rappoccio, B. Roozbahani

Northeastern University, Boston, USA

G. Alverson, E. Barberis, A. Hortiangtham, A. Massironi, D.M. Morse, D. Nash, T. Orimoto, R. Teixeira De Lima, D. Trocino, D. Wood

Northwestern University, Evanston, USA

S. Bhattacharya, O. Charaf, K.A. Hahn, N. Mucia, N. Odell, B. Pollack, M.H. Schmitt, K. Sung, M. Trovato, M. Velasco

University of Notre Dame, Notre Dame, USA

N. Dev, M. Hildreth, K. Hurtado Anampa, C. Jessop, D.J. Karmgard, N. Kellams, K. Lannon, N. Loukas, N. Marinelli, F. Meng, C. Mueller, Y. Musienko³⁶, M. Planer, A. Reinsvold, R. Ruchti, G. Smith, S. Taroni, M. Wayne, M. Wolf, A. Woodard

The Ohio State University, Columbus, USA

J. Alimena, L. Antonelli, B. Bylsma, L.S. Durkin, S. Flowers, B. Francis, A. Hart, C. Hill, W. Ji, B. Liu, W. Luo, D. Puigh, B.L. Winer, H.W. Wulsin

Princeton University, Princeton, USA

A. Benaglia, S. Cooperstein, O. Driga, P. Elmer, J. Hardenbrook, P. Hebda, S. Higginbotham,

D. Lange, J. Luo, D. Marlow, K. Mei, I. Ojalvo, J. Olsen, C. Palmer, P. Piroué, D. Stickland, C. Tully

University of Puerto Rico, Mayaguez, USA

S. Malik, S. Norberg

Purdue University, West Lafayette, USA

A. Barker, V.E. Barnes, S. Folgueras, L. Gutay, M.K. Jha, M. Jones, A.W. Jung, A. Khatiwada, D.H. Miller, N. Neumeister, C.C. Peng, J.F. Schulte, J. Sun, F. Wang, W. Xie

Purdue University Northwest, Hammond, USA

T. Cheng, N. Parashar, J. Stupak

Rice University, Houston, USA

A. Adair, B. Akgun, Z. Chen, K.M. Ecklund, F.J.M. Geurts, M. Guilbaud, W. Li, B. Michlin, M. Northup, B.P. Padley, J. Roberts, J. Rorie, Z. Tu, J. Zabel

University of Rochester, Rochester, USA

A. Bodek, P. de Barbaro, R. Demina, Y.t. Duh, T. Ferbel, M. Galanti, A. Garcia-Bellido, J. Han, O. Hindrichs, A. Khukhunaishvili, K.H. Lo, P. Tan, M. Verzetti

The Rockefeller University, New York, USA

R. Ciesielski, K. Goulios, C. Mesropian

Rutgers, The State University of New Jersey, Piscataway, USA

A. Agapitos, J.P. Chou, Y. Gershtein, T.A. Gómez Espinosa, E. Halkiadakis, M. Heindl, E. Hughes, S. Kaplan, R. Kunnawalkam Elayavalli, S. Kyriacou, A. Lath, R. Montalvo, K. Nash, M. Osherson, H. Saka, S. Salur, S. Schnetzer, D. Sheffield, S. Somalwar, R. Stone, S. Thomas, P. Thomassen, M. Walker

University of Tennessee, Knoxville, USA

A.G. Delannoy, M. Foerster, J. Heideman, G. Riley, K. Rose, S. Spanier, K. Thapa

Texas A&M University, College Station, USA

O. Bouhali⁷², A. Castaneda Hernandez⁷², A. Celik, M. Dalchenko, M. De Mattia, A. Delgado, S. Dildick, R. Eusebi, J. Gilmore, T. Huang, T. Kamon⁷³, R. Mueller, Y. Pakhotin, R. Patel, A. Perloff, L. Perniè, D. Rathjens, A. Safonov, A. Tatarinov, K.A. Ulmer

Texas Tech University, Lubbock, USA

N. Akchurin, J. Damgov, F. De Guio, P.R. Duderu, J. Faulkner, E. Gурpinar, S. Kunori, K. Lamichhane, S.W. Lee, T. Libeiro, T. Peltola, S. Undleeb, I. Volobouev, Z. Wang

Vanderbilt University, Nashville, USA

S. Greene, A. Gurrola, R. Janjam, W. Johns, C. Maguire, A. Melo, H. Ni, P. Sheldon, S. Tuo, J. Velkovska, Q. Xu

University of Virginia, Charlottesville, USA

M.W. Arenton, P. Barria, B. Cox, R. Hirosky, A. Ledovskoy, H. Li, C. Neu, T. Sinthuprasith, X. Sun, Y. Wang, E. Wolfe, F. Xia

Wayne State University, Detroit, USA

R. Harr, P.E. Karchin, J. Sturdy, S. Zaleski

University of Wisconsin - Madison, Madison, WI, USA

M. Brodski, J. Buchanan, C. Caillol, S. Dasu, L. Dodd, S. Duric, B. Gomber, M. Grothe,

M. Herndon, A. Hervé, U. Hussain, P. Klabbers, A. Lanaro, A. Levine, K. Long, R. Loveless, G.A. Pierro, G. Polese, T. Ruggles, A. Savin, N. Smith, W.H. Smith, D. Taylor, N. Woods

†: Deceased

- 1: Also at Vienna University of Technology, Vienna, Austria
- 2: Also at State Key Laboratory of Nuclear Physics and Technology, Peking University, Beijing, China
- 3: Also at Universidade Estadual de Campinas, Campinas, Brazil
- 4: Also at Universidade Federal de Pelotas, Pelotas, Brazil
- 5: Also at Université Libre de Bruxelles, Bruxelles, Belgium
- 6: Also at Institute for Theoretical and Experimental Physics, Moscow, Russia
- 7: Also at Joint Institute for Nuclear Research, Dubna, Russia
- 8: Also at Suez University, Suez, Egypt
- 9: Now at British University in Egypt, Cairo, Egypt
- 10: Also at Fayoum University, El-Fayoum, Egypt
- 11: Now at Helwan University, Cairo, Egypt
- 12: Also at Université de Haute Alsace, Mulhouse, France
- 13: Also at Skobeltsyn Institute of Nuclear Physics, Lomonosov Moscow State University, Moscow, Russia
- 14: Also at Tbilisi State University, Tbilisi, Georgia
- 15: Also at CERN, European Organization for Nuclear Research, Geneva, Switzerland
- 16: Also at RWTH Aachen University, III. Physikalisches Institut A, Aachen, Germany
- 17: Also at University of Hamburg, Hamburg, Germany
- 18: Also at Brandenburg University of Technology, Cottbus, Germany
- 19: Also at Institute of Nuclear Research ATOMKI, Debrecen, Hungary
- 20: Also at MTA-ELTE Lendület CMS Particle and Nuclear Physics Group, Eötvös Loránd University, Budapest, Hungary
- 21: Also at Institute of Physics, University of Debrecen, Debrecen, Hungary
- 22: Also at Indian Institute of Technology Bhubaneswar, Bhubaneswar, India
- 23: Also at Institute of Physics, Bhubaneswar, India
- 24: Also at University of Visva-Bharati, Santiniketan, India
- 25: Also at University of Ruhuna, Matara, Sri Lanka
- 26: Also at Isfahan University of Technology, Isfahan, Iran
- 27: Also at Yazd University, Yazd, Iran
- 28: Also at Plasma Physics Research Center, Science and Research Branch, Islamic Azad University, Tehran, Iran
- 29: Also at Università degli Studi di Siena, Siena, Italy
- 30: Also at INFN Sezione di Milano-Bicocca; Università di Milano-Bicocca, Milano, Italy
- 31: Also at Purdue University, West Lafayette, USA
- 32: Also at International Islamic University of Malaysia, Kuala Lumpur, Malaysia
- 33: Also at Malaysian Nuclear Agency, MOSTI, Kajang, Malaysia
- 34: Also at Consejo Nacional de Ciencia y Tecnología, Mexico city, Mexico
- 35: Also at Warsaw University of Technology, Institute of Electronic Systems, Warsaw, Poland
- 36: Also at Institute for Nuclear Research, Moscow, Russia
- 37: Now at National Research Nuclear University 'Moscow Engineering Physics Institute' (MEPhI), Moscow, Russia
- 38: Also at St. Petersburg State Polytechnical University, St. Petersburg, Russia
- 39: Also at University of Florida, Gainesville, USA
- 40: Also at P.N. Lebedev Physical Institute, Moscow, Russia
- 41: Also at California Institute of Technology, Pasadena, USA

- 42: Also at Budker Institute of Nuclear Physics, Novosibirsk, Russia
- 43: Also at Faculty of Physics, University of Belgrade, Belgrade, Serbia
- 44: Also at INFN Sezione di Roma; Sapienza Università di Roma, Rome, Italy
- 45: Also at University of Belgrade, Faculty of Physics and Vinca Institute of Nuclear Sciences, Belgrade, Serbia
- 46: Also at Scuola Normale e Sezione dell'INFN, Pisa, Italy
- 47: Also at National and Kapodistrian University of Athens, Athens, Greece
- 48: Also at Riga Technical University, Riga, Latvia
- 49: Also at Universität Zürich, Zurich, Switzerland
- 50: Also at Stefan Meyer Institute for Subatomic Physics (SMI), Vienna, Austria
- 51: Also at Istanbul University, Faculty of Science, Istanbul, Turkey
- 52: Also at Istanbul Aydin University, Istanbul, Turkey
- 53: Also at Mersin University, Mersin, Turkey
- 54: Also at Cag University, Mersin, Turkey
- 55: Also at Piri Reis University, Istanbul, Turkey
- 56: Also at Gaziosmanpasa University, Tokat, Turkey
- 57: Also at Adiyaman University, Adiyaman, Turkey
- 58: Also at Izmir Institute of Technology, Izmir, Turkey
- 59: Also at Necmettin Erbakan University, Konya, Turkey
- 60: Also at Marmara University, Istanbul, Turkey
- 61: Also at Kafkas University, Kars, Turkey
- 62: Also at Istanbul Bilgi University, Istanbul, Turkey
- 63: Also at Rutherford Appleton Laboratory, Didcot, United Kingdom
- 64: Also at School of Physics and Astronomy, University of Southampton, Southampton, United Kingdom
- 65: Also at Instituto de Astrofísica de Canarias, La Laguna, Spain
- 66: Also at Utah Valley University, Orem, USA
- 67: Also at Beykent University, Istanbul, Turkey
- 68: Also at Bingol University, Bingol, Turkey
- 69: Also at Erzincan University, Erzincan, Turkey
- 70: Also at Sinop University, Sinop, Turkey
- 71: Also at Mimar Sinan University, Istanbul, Istanbul, Turkey
- 72: Also at Texas A&M University at Qatar, Doha, Qatar
- 73: Also at Kyungpook National University, Daegu, Korea